SPHERE+: Reaching New Depths

A proposal to upgrade the instrument SPHERE at the VLT

Authors: A. Boccaletti[1] (spokeperson), O. Absil[2], S. Antoniucci[3], J.-C. Augereau[4], A. Baruffolo[5], J.-L. Baudino[1], P. Baudoz[1], M. Beaulieu[6], M. Benisty[4], J.-L. Beuzit[7], M. Bonnefoy[4], S. Bos[8], W. Brandner[9], F. Cantalloube[9], A. Carlotti[4], B. Charnay[1], G. Chauvin[4], E. Choquet[7], R. Claudi[5], J. de Boer[8], S. Desidera[5], P. Delorme[4], D. Doelman[8], K. Dohlen[7], C. Dominik[10], V. D'Orazi[5], N. Engler[11], M. Feldt[9], T. Fusco[12], R. Galicher[1], A. Ghedina[13], C. Ginski[8], D. Gratadour[1], R. Gratton[5], C. Keller[8], M. Kenworthy[8], J. Kuhn[11], S. Haffert[8], T. Henning[9], M. Houllé[7], E. Huby[1], E. Lagadec[6], M. Langlois[14], A.-M. Lagrange[4], H. Le Coroller[7], G. Li Causi[3], A.L. Maire[2], F. Martinache[6], F. Ménard[4], D. Mesa[5], N. Meunier[4], J. Milli[4], D. Mouillet[4], L. Mugnier[12], M. N'Diaye,[6], G. Otten[7], P. Patapis[11], F. Pedichini[3], E. Por[8], A. Potier[1], S. Quanz[11], D. Rouan[1], M. Samland[9], J.-F. Sauvage[12], H.-M. Schmid[11], D. Segransan[15], G. Singh[1], F. Snik[8], M. Stangalini[3], M. Tallon[14], M. Turatto[5], S. Udry[15], R. Van Holstein[8], A. Vigan[7], F. Wildi[15], + SPHERE consortium

Institutes: (1) LESIA, Obs. Paris; (2) STAR, Univ. Liège; (3) INAF, Obs. Roma; (4) IPAG, Univ Grenoble-Alpes; (5) INAF, Obs. Padova; (6) Lagrange, Obs. Côte d'Azur; (7) LAM, Univ. Aix-Marseille; (8) NOVA, Univ. Leiden; (9) MPIA; (10) NOVA, Univ. Amsterdam; (11) ETH Zurich; (12) ONERA; (13) INAF, Centro Galileo Galilei; (14) CRAL, Univ. Lyon; (15) Obs. Genève

Contents

1 Introduction

In the coming years, the Very Large Telescope (VLT) will enter a new phase of operation with the implementation of its third generation of instruments (ERIS, MOONS and MAVIES), and the advent of the Extremely Large Telescope (ELT) in the second half of the 2020s. The VLT, together with the ELT, must maintain its world-leading position for the upcoming decade based on an adequate mid/long-term strategy offering high performance and versatile workhorse instruments, but also novel capabilities to serve a large community with the best scientific data. In this document we propose a significant upgrade to the Spectro-Polarimetric High-Contrast Exoplanet Research instrument (SPHERE[1], Beuzit et al. 2019), installed at UT3 since May 2014 (First Light, ESO-PR1417), so that SPHERE can remain unique and performant at the horizon 2030.

SPHERE has now been in operation at the VLT for more than 5 years, with a high level of performance and producing outstanding results using a variety of operating modes. SPHERE has been designed to optimally suppress the stellar light without removing the planetary signal using high-contrast and high-angular resolution techniques. To compensate for the atmospheric turbulence, SPHERE is equipped with an extreme adaptive optics (xAO) system to attain (under good seeing conditions and a moderate field of view) the ultimate spatial resolution of the telescope, and minimize the scattered light generated by its aberrations. Then, combining various techniques of coronagraphy and differential imaging, SPHERE can image young giant exoplanets and characterize them in great detail. The quality of the instrument has allowed a large community to obtain breakthrough scientific results, including the discovery and the characterization of new young exoplanets (ESO-ANN17041, ESO-PR1821), the detailed study of young solar systems in formation (ESO-PR1538, ESO-PR1640, ESO-PR1811), and evolved stars surroundings (ESO-PR1523, ESO-PR1840), the high resolution mapping of solar system bodies (ESO-POTW1749 and 1826), or even active galactic nuclei in NGC1068[2]. Thanks to this detailed understanding of its performance, the SPHERE instrument is one of arguably the best existing and operating xAO instrument worldwide.

The SPHERE+ concept described in this document aims at opening a new and meaningful scientific window for the upcoming decade in synergy with ground-based facilities (VLTI/I, ELT, ALMA, and SKA) and space missions (*Gaia*, *JWST*, *PLATO* and *WFIRST*). It also intends to maintain the leadership of ESO in the exoplanetary field. We identify three key scientific requirements that are currently driving this project as well as our proposed instrumental concept. They can be summarized as follows (Sec. 3 for details):

- `sci.req.1` - To access the bulk of the young giant planet population around the snow line (3-10 au), to bridge the gap with complementary techniques (radial velocity, astrometry), and to explore for the first time the complete demography of young giant planets at all separations to constrain their formation and evolution mechanisms.

- `sci.req.2` - To observe a large number of fainter (lower mass) stars in the youngest ($1-10$ Myr) associations (Lupus, Taurus, Chamaeleontis, Scorpius-Centaurus...), to directly study the formation of giant planets in their birth environment, building on the synergy with ALMA to characterize the architectures and properties of young protoplanetary disks, and how they relate to the population of planet observed around more evolved stars

- `sci.req.3` - To improve the level of characterization of exoplanetary atmospheres by increasing the spectral resolution to break degeneracies in giant planet atmosphere models, to measure abundances and other physical parameters, such as the radial and rotational velocities.

[1] `http://sphere.osug.fr`

[2] They represent a total of 110 articles in refereed publications for the SPHERE Guaranteed Time Observations and the Science Verification Time (GO not included).

Overall, the SPHERE+ top level requirements connected to the proposed science cases can be summarized by going **closer**, **deeper**, and **fainter**. They can be turned into the following instrumental requirements (Sec. 4 for details):

- `tech.req.1` - Deeper/closer: increase the bandwidth of the xAO system (typically 3kHz instead of 1kHz) and improve the correction of non-common path aberrations and coronagraphic rejection.
- `tech.req.2` - Fainter: include a more sensitive wavefront sensor to gain 2-3 magnitudes for red stars.
- `tech.req.3` - Enhanced characterization: develop spectroscopic facilities with significantly higher spectral resolution compared to the current SPHERE Integral Field Spectrograph (IFS). In this respect, both medium ($R_\lambda = 5000$) and high ($R_\lambda = 50000$) resolution are considered extremely valuable for the characterization of planetary atmospheres.

Another important item is the preparation for ELT instrument development. Increasing xAO performance at the VLT and testing new concepts (coupling high contrast and high spectral resolution) is mandatory in the ELT framework for future instruments, in particular any ELT instrument with ultimate capability to image and characterize the lightest planets (e.g. Super Earths). At the same time, it is recognized that the current version of SPHERE operates efficiently and smoothly with a good level of performance and a high rate of publications in various scientific areas. Therefore, the SPHERE+ project must have a limited impact on the system and the operating downtime of the instrument.

After a brief introduction of the pre-SPHERE context and today's SPHERE achievements, the scope of this document is to detail the science goals of the SPHERE+ project, the technical requirements to achieve these goals, and a general plan for the SPHERE+ implementation in the coming years. Such proposed implementation will be made without breaking the current operating scheme (low risk, possible roll back), with a minimal instrumental impact (modules fully tested consistently before insertion into the instrument and short commissioning times), and will offer a major gain in performance necessary to open a new scientific regime, in parallel with present and future space and ground-based facilities.

2 Pre-SPHERE context and achievements

2.1 The advent of Direct Imaging

Today's heritage in direct imaging (DI) of exoplanets is intimately connected to the pioneer work (particularly at ESO) in the late 80's and early 90's for the development of Adaptive Optics (AO) systems, infrared (IR) detectors, and coronagraphic techniques for the instrumentation of ground-based telescopes. The COME-ON AO prototype (that later became the ESO 3.6m/ADONIS instrument), the Johns Hopkins University AO Coronagraph, or the CFHT CIRCUS coronagraphic camera at CFHT, were precursor instruments that soon motivated the research and development of more sophisticated AO high-contrast imagers on 10m-class telescopes (LMIRCAM at LBT, PALAO-PHARO at Palomar, CIAO at Subaru, NIRC2 at Keck, NaCo at VLT, and NIRI and NICI at Gemini), confirming that ground-based instrumentation had demonstrated performances that could compete and develop synergies with space and *HST*. Following the discovery of the first brown dwarf GD165 B (Zuckerman & Becklin 1992), the power of combining improved angular resolution and high-contrast techniques was well envisioned for the discovery and characterization of substellar companions, including exoplanets, and protoplanetary and debris disks. The early emblematic discoveries and images of Gl229 B (Nakajima et al. 1995) and the β Pictoris disk (Mouillet et al. 1997) supported and motivated this approach even more (see Figure 1). Since the dawn of exoplanet discoveries in radial velocity in 1995,

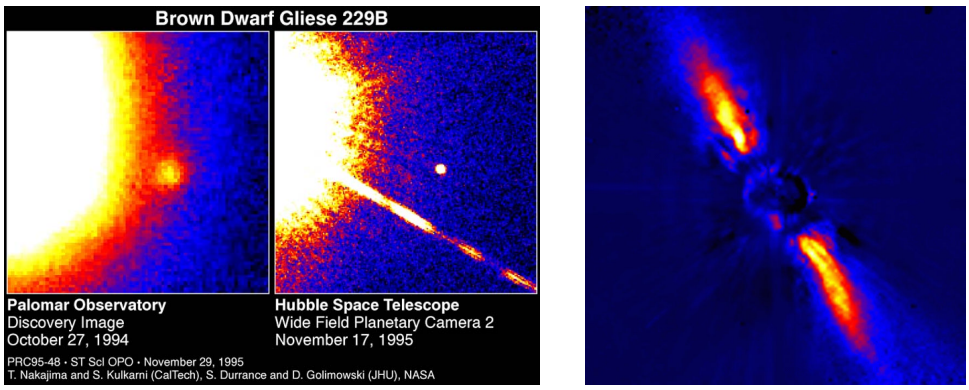

Figure 1: *Left,* Discovery image of the cool brown dwarf companion Gliese 299 B with the Johns Hopkins University AO Coronagraph at Palomar and with the *HST*/WFPC2 follow-up observation by Nakajima et al. (1995). *Right,* ESO3.6m/ADONIS coronagraphic observation of the edge-on debris disk around β Pictoris (Mouillet et al. 1997).

DI exploited the angular resolution and sensitivity of 10m-class telescopes in the early 2000s to join the small family of planet hunting techniques known nowadays with radial velocity, transit, μ-lensing and astrometry.

The first generation of planet imagers on 10m-class telescopes at Palomar, MMTO, Subaru, Keck, VLT, Gemini, followed by LBT and Magellan, enabled large systematic surveys of young, nearby stars. These surveys rapidly led to the discovery of the first planetary mass companions in the early 2000s with 2M1207b with NaCo at VLT (Chauvin et al. 2004, ESO-PR0515). Most of these were detected at large distances ($>$ 100 au) or with a small mass ratios relative to their stellar host, indicating a probable formation via gravo-turbulent fragmentation or gravitational disk instability. The implementation of differential techniques, starting in 2005–2006, led to the breakthrough discoveries of closer and lighter planetary mass companions like HR 8799 bcde, (Marois et al. 2010), β Pictoris b (Lagrange et al. 2009), GJ 504 b (Kuzuhara et al. 2013), and HD 95086 b (Rameau et al. 2013), initiating the era of a more systematic characterization of the giant planet population at wide orbits, between typically 5 and 100 au.

Nowadays, DI brings a unique opportunity to explore the outer part of exoplanetary systems beyond 5 au to complete our view of planetary architectures, and to explore the properties of relatively cool giant planets. The exoplanet's photons can indeed be spatially resolved and dispersed to probe directly the atmospheric properties of exoplanets (and brown dwarf companions). As today's imaged exoplanets are young (because they are hotter, brighter, thus easier to detect than their older counterparts), their atmospheres show low-gravity features, as well as the presence of clouds, and non-equilibrium chemistry processes. These physical conditions are very different and complementary to the ones observed in the atmospheres of field brown dwarfs or irradiated inflated Hot Jupiters (studied in standard spectroscopy and with transit techniques like transmission and secondary-eclipse spectroscopy, respectively). Finally, DI enables to directly probe the presence of planets together with their environment of formation. Planetary characteristics and disk spatial structures can then be linked to study the planet – disk interactions and the planetary system's formation, evolution, and stability, which is a fundamental and inevitable path to understand the formation of smaller telluric planets with suitable conditions to host life.

2.2 SPHERE discoveries and achievements

The success of SPHERE is related to its sophisticated instrumentation optimized for the detection of faint planetary signals at small angular separations from a bright star. A planet orbiting at 9 au around

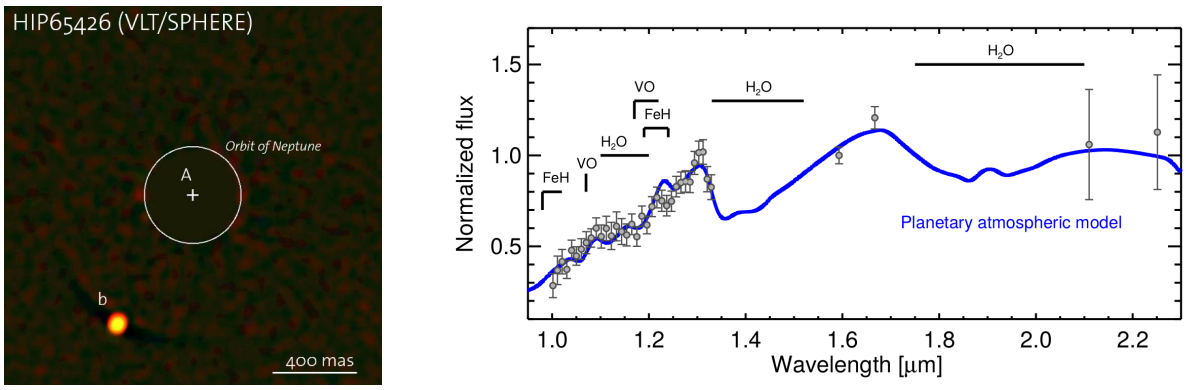

Figure 2: *Left,* Composite IFS YJ-band and IRDIS H2H3 TLOCI image of HIP 65426 A and b from February, 2017. The first planet discovered with SPHERE is well detected at a separation of 830 ± 3 mas and position angle of 150.0 ± 0.3 deg from HIP 65426. *Right,* Near-infrared spectrum of HIP 65426 b extracted with the TLOCI algorithm compared with the best-fit model atmosphere from the Exo-REM atmospheric model in blue ($T_{\rm eff} = 1660$ K, $log(g) = 4.5$, $f_{\rm sed} = 1.5$, and $R = 1.5\,R_{\rm Jup}$).

a star at 30 pc distance lies at a maximum angular separation of 300 mas, which defines our typical angular separation. As young planets are still warm, the star-planet contrast for a solar type star and a Jupiter-mass planet is $\sim 10^{-6}$, while for a mature (cold) Jupiter the contrast increases to 10^{-8} at best (i.e. at the peak of its spectral energy distribution). For a super-Earth observed in reflected light, the planet-star contrast increases to 10^{-9}. Compared to the early discoveries of young and massive self-luminous giant planets like β Pictoris b (H-band contrast of 10^{-4} at 400 mas) with NaCo at the VLT, imaging of telluric planets with the ELT will require several orders of magnitude higher contrast at a factor of 5 to 10 smaller angular resolution. Innovative technological developments are therefore required to meet these ultimate goals. SPHERE brought a significant gain in performance compared to the first generation of planet imagers and now routinely achieves high-contrast performances down to 10^{-5}–10^{-6} at typical separations of 300 mas. These results now validate the decisions made more than 10 years ago about a dedicated design based on a 3-stage implementation: i/ high angular resolution using xAO, ii/ stellar light attenuation using coronagraphy, and iii/ speckle subtraction using differential imaging techniques (angular, spectral, and polarimetric). A fourth step can be added with the development of powerful post-processing tools (iv/) to optimize the stellar signal suppression. They support the early motivation for systematic and large scale surveys to exploit SPHERE outstanding performances to search for exoplanets and disks around a large sample of young, nearby stars.

2.2.1 Exoplanets

Following the first light of SPHERE in May 2014, vast efforts have been devoted during the early phase of operation on the characterization of several known young planetary systems to highlight the SPHERE detection, astrometric and spectro-photometric performance. Among the systems characterized, we can list the most ultracool brown dwarf companions ever imaged around GJ 758, GJ 504 and HD 4113 (Vigan et al. 2016; Bonnefoy et al. 2018; Cheetham et al. 2018b), the young highly-eccentric brown dwarf companion around PZ Tel (Maire et al. 2016), the spectroscopic characterization of the reddest substellar companion discovered so far HD 206893 B (Delorme et al. 2017b) and of the newly discovered cool giant planet 51 Eri b (Samland et al. 2017), or the orbital and dynamical study of the young solar-system analogs architecture of HR 8799 (Zurlo et al. 2016; Bonnefoy et al. 2016) and HD 95086 (Chauvin et al. 2018). These first studies paved the path toward the first SPHERE exoplanet discovery of a warm, dusty and cloudy massive Jupiter around the young Lower-Centaurus

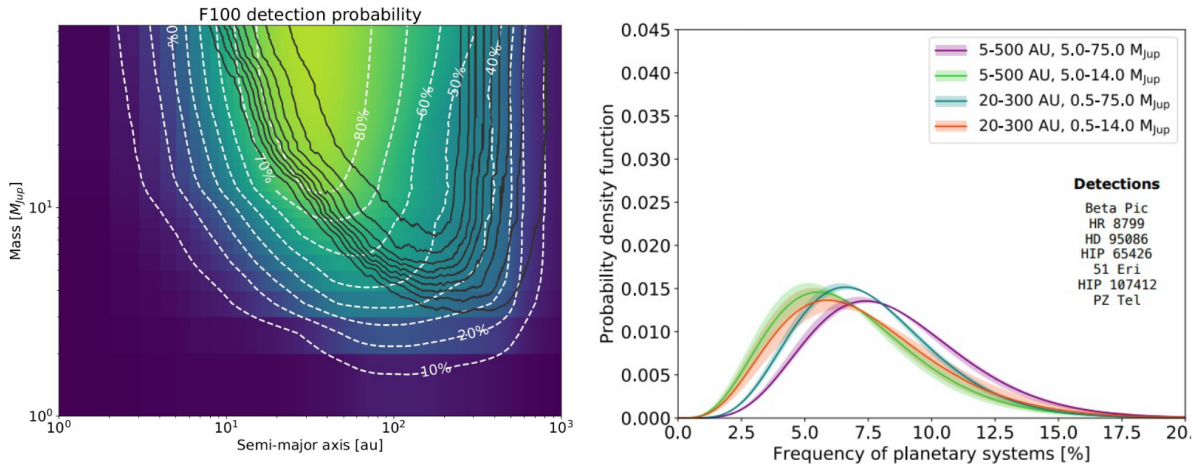

Figure 3: *Left,* SPHERE SHINE survey completeness for the early sample of 175 stars observed during the first years of operation. The NaCo Large Program completeness is reported in black for comparison. *Right,* Frequency of the planet and planet-brown dwarf population at separations largers than 5 au as observed by SPHERE SHINE.

Crux association member HIP 65426 (Chauvin et al. 2017, ESO-ANN17041), which was followed by the first unambiguous discovery of a young planet recently formed within a transition disk and orbiting the young star PDS 70 (Keppler et al. 2018; Müller et al. 2018, ESO-PR1821). These latest breakthrough results shed light on SPHERE capabilities and directly brought a worldwide recognition in the exoplanetary research field. After 5 years of operation, the key SPHERE achievements in this domain can be summarized as follows:

- Physics of exoplanets: in addition to the discovery of new exoplanets, SPHERE acquired unprecedented near-infrared photometry and spectra of young giant planets, enabling the exploration of the physical processes at play in their atmospheres (see Figure 2). The early characterization of the HR 8799 d and e planets by Zurlo et al. (2016) and Bonnefoy et al. (2016) show the peculiar properties of young L/T type planets owing to the low-surface gravity conditions in their atmospheres, leading to an enhanced production of dust forming thick clouds composed of sub-μm grains made of corundum, iron, enstatite, or forsterite, successfully reproduce the spectral energy distributions of these planets. Similar trends were found for the young planets 51 Eri b, HIP 65426 b, HD 95086 b, and PDS 70 b (Samland et al. 2017; Cheetham et al. 2019; Chauvin et al. 2018; Müller et al. 2018). They were complemented by spectral characterization of young brown dwarf companions, such as HR 3549B, HR 2562 B or HIP 64892 (Mesa et al. 2016, 2018; Cheetham et al. 2018a). Thanks to SPHERE, we are now building a detailed spectral sequence of young brown dwarves and exoplanets extending from late-M to T-types that allows to explore the effect of effective temperature, surface gravity (pressure), composition, clouds, and thermodynamical instabilities in the atmospheres of substellar objects down to young Jupiter analogs.

- Planetary architectures: At young ($\lesssim$ 10 Myr) ages, the presence of cavities, spirals, and kinematic perturbations in protostellar disks are likely to be caused by protoplanets in formation. In HD 169142, we identified several structures in Keplerian motion, blobs, spiral arms and one potential planet in formation (Gratton et al. 2019a). At ages greater than 10 Myr, the gas is expected to have dispersed, giant planets to have formed and the dynamics of planetesimals to be influenced by the presence of giant planets. The combination of high contrast performances and astrometric precision at level of 1-2 mas, provided by SPHERE, enable accurate monitoring

of the planet position over time. It offers the rich possibility to study, in addition to the planet's orbit, the global system architecture including the planet-planet and planet-disk interactions and the system stability. A landmark case for such configuration is β Pictoris. The orbital monitoring of β Pictoris b - combining NaCo and SPHERE - enabled continuous monitoring of the planet's orbit around its star, passing behind the star from a North-East location to South-West, reaching quadrature in Summer 2013 and moving toward North-East afterwards. The planet was observed down to 130 mas in projected separation in Fall 2016 and recovered at 150 mas in Fall 2018, after its passage in front of the star. To our knowledge, no other instrument could reach such a high contrast capability (Lagrange et al. 2019, ESOcast-183). The accurate orbital follow-up confirms that the planet is shaping the inner warp of the circumstellar disk and is responsible for the exocometary activity known for decades. Similar studies have been conducted for the young solar analogs HR 8799 and HD 95086 (Zurlo et al. 2016; Chauvin et al. 2018) or even HR 2562 (Maire et al. 2018). Here again, the planet physical and orbital properties can be compared to the dust spatial distribution and architecture, and show configuration very similar to the one of our solar system (with the asteroid and the Kuiper belts separated by the existence of giant planets). These systems provide precious laboratories to understand the formation of our own solar system and even life.

- Occurrence & formation: With the large number of exoplanet discoveries since the 51 Peg b announcement, the theories of planetary formation have drastically evolved to digest these new observational constraints. However, we are still missing the full picture and some key fundamental questions still lack answers, such as the physics of accretion to form planetary atmospheres, the formation and evolution mechanisms to explain the existence of giant planets at wide orbits, the physical properties of young Jupiters, or the influence of the stellar mass and stellar environment in the planetary formation processes. Neither core accretion plus gas capture (CA) nor disk fragmentation driven by gravitational instabilities (GI) can globally explain all current observables from planet hunting techniques. However, we are still lacking a global view of the occurrence of exoplanets at all orbital periods. In this context, the SpHere INfrared survey for Exoplanets (SHINE) of 600 stars from the SPHERE Guaranteed Time Observations (GTO) is providing unique statistical constraints on the demography of giant planets beyond 5 au (see the mean survey detection probability in Figure 3 compared to the one of the first generation of planet imagers). The early statistical results confirm a rather low frequency of planetary systems hosting at least one giant planet between 5 to 500 au with an estimated value of 5% for massive giant planets (to be consolidated at the end of the survey). The size and properties of the SHINE sample should enable to study the variation of the occurrence with the stellar mass and age. The SHINE survey completeness will also be directly compared to the current predictions of planetary formation models to test the efficiency of each physical process at play (see Vigan et al. 2017), and will be combined with the picture given by complementary techniques (transit, radial velocity, μ-lensing and astrometry) to offer a global vision of planet occurence at all separations.

2.2.2 Circumstellar disks

One of the greatest achievements of SPHERE resides in the number of studies regarding the fine structures of imaged circumstellar disks, revealing unprecedented information about the structure of planetary systems during or right after the planetary formation phase (Fig. 4 and Fig. 5). SPHERE has observed two types of disks, protoplanetary disks ($\lesssim 10$ Myr) where both gas and dust are present in which we expect planets are still forming, and debris disks ($\gtrsim 10$ Myr), which are dominated by second generation dust (from collisions between planetesimals) and where planets are already formed. The efficiency of SPHERE in the context of circumstellar disks relies on a large enough field of view and two main observing modes allowing total intensity and polarized intensity imaging both in the

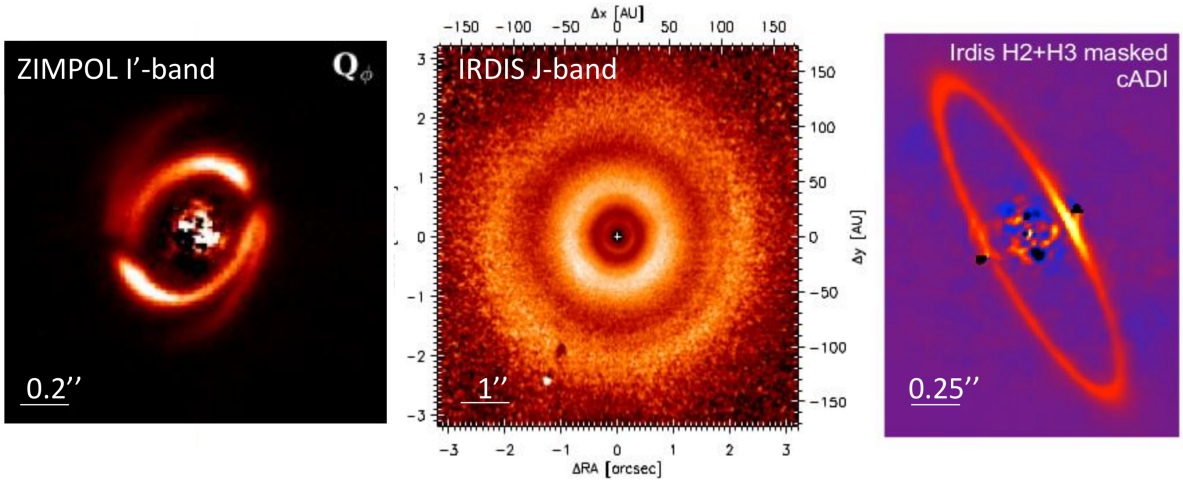

Figure 4: Typical structures observed in protoplanetary and debris disks. *From left to right*: large spirals and shadows in the transition disk of HD 100543 (Benisty et al. 2017), gaps and thin spiral in the transition disk of TW Hya (van Boekel et al. 2017), and, a Kuiper-like belt of planetesimals in the debris disk of HR4796 (Milli et al. 2017).

visible and near IR. With these capabilities, we were able to resolve new structures in known disks, to obtain the first images of disks suspected from their IR excess, and to serendipitously discover new disks (see below).

The main outcome of disk science with SPHERE is certainly the many structures that were spatially resolved and in some cases characterized spectroscopically or polarimetrically. Among the most emblematic results, SPHERE has discovered: large spiral arms (MWC 758, Benisty et al. 2015), multiple rings or gaps (TW Hya, RXJ 1615, HD 97048, van Boekel et al. 2017; de Boer et al. 2016; Ginski et al. 2016), variable shadows (SAO 206462, V4046 Sgr, Stolker et al. 2016; D'Orazi et al. 2019), central cavities (HD 169142, PDS 70, Pohl et al. 2017; Ligi et al. 2018; Keppler et al. 2018) in protoplanetary disks. For what concerns debris disks, SPHERE has also resolved several sharp Kuiper-like belts (HD 106906, HR 4796, HD 114082, GSC 07396-00759, Lagrange et al. 2016; Milli et al. 2017; Wahhaj et al. 2016; Sissa et al. 2018), multiple belts in gas-rich debris disks (HD 61005, HD 141956A, HIP 73145, HIP 67497, Olofsson et al. 2016; Perrot et al. 2016; Feldt et al. 2017; Bonnefoy et al. 2017) and moving structures (AU Mic, Boccaletti et al. 2015, 2018). The vast majority of these structures could be explained by the presence of planets (Dong et al. 2015b,a; Lee & Chiang 2016; Sezestre et al. 2017) or by massive collisions (Jackson et al. 2014; Kral et al. 2015). All these results have contributed to reinforce the fact that disk science is closely connected to exoplanet science, the case of PDS 70 b, where a planet was discovered right inside the cavity, being definitely the best example. Spectral and polarimetric informations collected by SPHERE also played an important role in putting constraints on dust properties (size distribution for instance or mineralogy). In only 5 years, the contribution of SPHERE to disk science is already impressive with a total of 50 disks resolved for the first time in scattered light, and about 60 related papers have been published, strengthened by a very strong synergy with ALMA. In fact, SPHERE has been able to image for the first time 11 debris disks (out of 45 known, i.e. 25%) and 39 protoplanetary disks (out of the 200 known in nearby star forming regions, i.e. 20%), hence competing (in only 5 years!) with *HST* which achieves a better sensitivity at large separations, but poorer angular resolution.

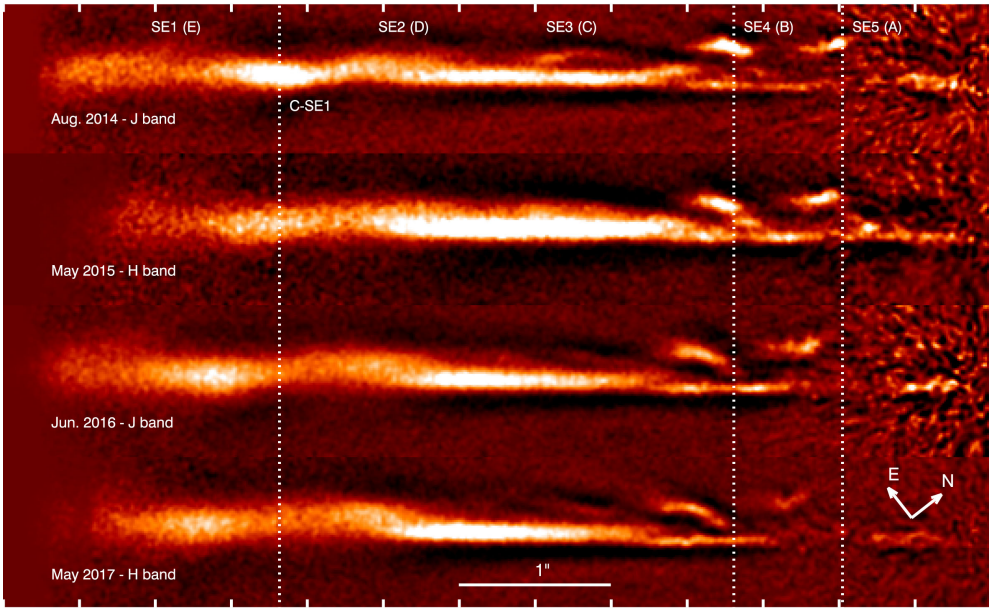

Figure 5: Fast moving structures observed in the debris disk of AU Mic, from Aug. 2014 to May 2017, and possibly triggered by the action of the stellar wind on an undetected planet or a reservoir of dust (Boccaletti et al. 2018).

2.2.3 Galactic, stellar, and solar system physics

Although SPHERE was designed to image planets and disks, its sophisticated instrumentation led to breakthrough discoveries for a broad variety of astrophysical topics including galactic, stellar and solar system physics.

For instance, SPHERE obtained revolutionary results for the study of the late stages of stellar evolution characterized by a very large mass loss, leading to the chemical enrichment of the Galaxy and to a final fate for the stars. This mass loss is poorly understood, and certainly the combination of convection, pulsation, dust and molecule formation and radiation pressure. The resolution achieved with ZIMPOL (20 mas), combined with its polarimetric capabilities (enabling the detection of dusty clumps) were the key to directly image the surface of a few giant stars, such as Betelgeuse (Kervella et al. 2016) and R Doradus (Khouri et al. 2016). They also mapped gas next to the surface of stars and showed that the molecular opacity was time-dependent, and certainly due to the formation of molecules above convective cells. The formation of these molecules and shocks due to a combination of pulsation and convection can lead to dust formation, as observed for W Hya (Ohnaka et al. 2017) and Mira Ceti (Khouri et al. 2018). For oxygen-rich stars, SPHERE showed for the first time that the silicate grains around evolved stars are large (micron-sized), and that the mass loss can be explained by scattering by large grains such as observed for VY CMa (Scicluna et al. 2015) and W Hya (Ohnaka et al. 2016). It led to a significant better understanding of the impact of companions on the mass loss from these evolved stars as most stars are born in multiple systems. This was illustrated by the mapping with unprecedented details of the dusty spiral formed by the interaction of an emblematic Wolf Rayet star with its O star companion in WE 104 (Soulain et al. 2018) or observations of the prototypical symbiotic system (an interacting binary system with an AGB star and a compact companion) R Aquarii resolved, for the first time, with its binary companion and a precessing jet due to their interlace interaction (Schmid et al. 2017). Finally, for the nearby AGB star L2 Puppis, SPHERE managed to resolve a close companion and clear signs of interactions with the formation of an equatorial disc with ejection of plumes perpendicular to it (Kervella et al. 2015). This is the first direct image of the precursor of the spectacular butterfly planetary nebulae and this certainly represents the future of our own solar system.

SPHERE also provided the first direct insights on the launching region of jets from young stars, which is crucial for determining their feedback on the disk and requires probing distances within a few au from the driving source (tens of mas for close-by YSOs). In particular, Antoniucci et al. (2016) observed the jets from Z CMa, deriving a first direct mass loss rate estimate for a FUor object and detecting a wiggling possibly indicative of an unseen close-in companion, while Garufi et al. 2019 (in press) analyzed the jet from RY Tau and its interaction with the complex circumstellar structures of the source.

The unique capabilities of SPHERE, and in particular ZIMPOL opened new doors in ground-based asteroid exploration, namely, geophysics and geology. It indeed enabled to obtain resolved images of the surfaces of asteroids. Making use of the rotation of these objects and 3D modeling, the accurate shapes (and volumes) of asteroids have been determined. For asteroids in binary systems, this can lead to an accurate mass (and thus density) determination. Comparisons with results from on site space missions show that one can study with great accuracy the topography and albedo of asteroids using ZIMPOL (see e.g. the Vesta observations by Fétick et al. 2019). More and more asteroids are being resolved to determine their 3D shapes (Elektra, Hanuš et al. 2017; Julia, Vernazza et al. 2018; Daphne, Carry et al. 2019; Hebe, Marsset et al. 2017; (3) Juno, Viikinkoski et al. 2015 (16) Psyche, Viikinkoski et al. 2018). Studying the density and surface craters of these asteroids enabled, for the first time, to study from the ground the geology of these asteroids and better understand their formation and their parent bodies and families.

Finally, the angular resolution and sensitivity reached by SPHERE enabled to improve our knowledge of stellar clusters and AGNs. Khorrami et al. (2016) studied the core of the young massive cluster NGC 3603, to show that its central mass function was different than previously assumed, as previous studies were limited by crowding and the lack of dynamic range. Observation of the extragalactic cluster R136 showed that the stars thought to be the most massive in the Universe had optical companions, and that their mass was certainly overestimated (Khorrami et al. 2017). Finally, the circumnuclear optically thick material hiding the central core of the Active Galactic Nuclei NGC 1068 was mapped with SPHERE. They show strong evidence that there is an extended nuclear torus at the center of NGC 1068 (Gratadour et al. 2015). There is a structured hourglass-shaped bicone and a compact elongated (20×60 pc) nuclear structure perpendicular to the bicone axis.

SPHERE is thus a very versatile instrument, able to tackle a large variety of key questions including various ones that were not anticipated as the first determination of the mass of Proxima Cen from a microlensing event (Zurlo et al. 2018). These observations of targets other than planets and disks led to stunning images, outlined by 4 ESO press-releases (R Aqr, ESO-PR1840; Asteroids, ESO-PR1910; VY Cma, ESO 1546; L2 Pup, ESO-PR1523; and 4 pictures of the week (Ceres, ESO-PR1536; Asteroids, ESO-PR1725; Titan, ESO-PR1417; Vesta, ESO-PR1826). A SPHERE+ instrument will considerably expand the possibilities offered in galactic, stellar and solar system physics by reaching closer separations and deeper contrasts, fainter targets, and higher spectral resolution.

3 Science goals

3.1 Exoplanetary science

3.1.1 Demography of giant planets: bridging the gap (`sci.req.1`)

(1) How does the bulk of the close-in giant planet population observed in transit and radial velocity surveys extend?

In Figure 3, we have seen that with the current SPHERE detection performances we are routinely able to achieve a (5σ) contrast detection limit of 10^{-5} at 300 mas in near-infrared. It translates into the ability to explore the population of giant planets located between 10 to 300 au with masses typically

larger than 2 $M_{\rm Jup}$ when considering a sample of young, nearby stars. The early statistical results of the SHINE campaign indicate that the rate of discovery in this parameter space remains relatively low despite the large number of stars observed and shows that the bulk of the massive giant planet population observed in radial velocity, and located between 2 - 8 au, does not seem to extend much beyond 10 au. The overlap between radial velocity (soon astrometry with *Gaia*) and DI is nowadays marginal (Lannier et al. 2017; Lagrange et al. 2018), and a prime scientific goal of the SPHERE+ project will be to bridge that gap to exploit the synergies between these techniques in order to obtain a complete view of the demography of the giant planet population at all separations (see Figure 6). This will enable to further constrain the distributions of masses and orbital properties of giant planets to test the theories of planetary formation and evolution.

(2) Mass - Luminosity relationship to tackle the early phases of formation and evolution of young Jupiters for the first time!

A second very important scientific goal will be to build on this synergy to further explore the physical properties of young Jovian planets, which remain highly uncertain at young ages. DI gives access to the photometry, the luminosity and the spectral energy distribution of exoplanets, but not directly to the mass. In this context, we have to rely on evolutionary model predictions that are not well calibrated at young ages. In addition to the system age uncertainty, the predictions highly depend on the formation mechanisms and the gas-accretion phase that will form the exoplanetary atmosphere. The way the accretion shock will behave (sub or super-critical) on the surface of the young accreting proto-planets during the phase of gas runaway accretion will drive the initial entropy or internal energy, hence its initial physical properties (luminosity, effective temperature, surface gravity and radius) and their evolution with time. These different physical states are described by the so-called hot-start (sub-critical shock), cold-start (super-critical shock), and warm-start (intermediate case) models. They predict luminosities that are spread over several orders of magnitudes for young, massive giant planets. This is illustrated by the Figure 5 of the BEX models from Mordasini et al. (2017) for instance, where predictions in terms of luminosity are reported for different planet masses as a function of time and for the cold-start and hot-start cases. The higher the mass, the larger the spread and the time duration for the models to converge. Nowadays, most masses reported in the literature for imaged planets are the ones predicted by hot-start models and may under-estimate the planet masses as they fail to capture the accretion processes at play for the formation of giant planet atmospheres.

Getting closer and deeper to access physical separations down to 3 au (100 mas) with a typical (5σ) contrast of 10^{-5} to carry out the science described above requires:

- Systematic survey of the young, nearby stars observed during the SHINE campaign but at closer physical separations to explore the demography of giant planets beyond 3 au. SPHERE+ will serve here as a survey instrument providing further statistical constraints on the occurrence and distributions of giant planets in overlap with complementary techniques as radial velocity and astrometry. There is a clear synergy with the ELT that will not be able to devote a large amount of nights for large systematic surveys. The new exoplanetary systems that will be discovered and imaged by SPHERE+ will be prime targets for in-depth characterization with the ELT. Carrying this survey in service observing mode would be particularly important to take advantage of the best seeing and coherence time conditions to optimize the SPHERE+ exploitation.
- Imaging and characterizing the young giant planets that will be discovered with *Gaia* in the context of the Data Release 4 (2022) and in the course of radial velocity campaigns targeting young, nearby stars with HARPS/3.6m, NIRPS/3.6m, ESPRESSO at VLT.

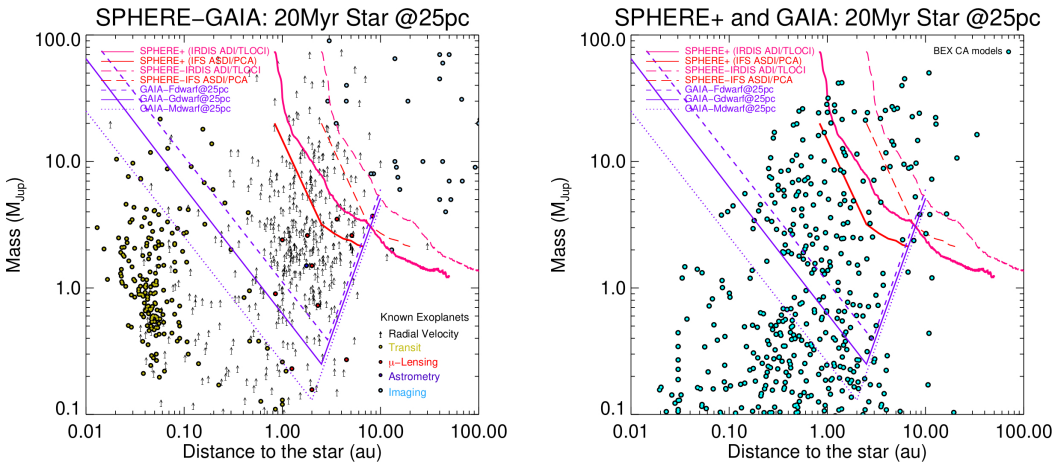

Figure 6: *Left,* SPHERE and expected SPHERE+ detection limits for a young (20 Myr), nearby (25 pc) star compared to the current population of exoplanets detected with all techniques (DI, transit, radial velocity, μ-lensing and astrometry) and the *Gaia* detection limits that will be available with the Data Release 4 in 2022. *Right,* SPHERE, SPHERE+ and *Gaia* DR4 detection limits compared to the prediction of the BEX Core Accretion models from Mordasini et al. (2017).

3.1.2 New insight on physical properties of young Jupiters and boosted detection capabilities (`sci.req.3`)

(1) Towards the exploration of new physical properties of giant planets: accretion rates, surface gravity, metallicity, composition, abundances, clouds properties and coverage, and rotational period.

Exoplanetary atmosphere studies were initiated more than a decade ago with the atmospheric characterization of hot and strongly irradiated Jupiters like HD 209458 b (Charbonneau et al. 2002) using transit observations. Such observations have been reported for over 30 exoplanets to date (Seager & Deming 2010), including hot Jupiters, hot Neptunes (e.g. Stevenson et al. 2010), and even super-Earths (Demory et al. 2012). Nowadays, three main observing techniques are currently used to study the atmosphere of exoplanets: low/medium resolution spectroscopy in transmission during transit or in emission using secondary eclipse, high-dispersed spectroscopy, and high contrast low-resolution spectroscopy. The last technique has been used in DI to acquire the first spectra of non-strongly irradiated and self-luminous Jovian planets in wide orbits to enable the detailed physical and chemical characterization of their atmosphere with a possible link to their processes of formation (Janson et al. 2011; Konopacky et al. 2013; Bryan et al. 2018).

Today's low spectral ($R_\lambda = 30 - 50$) resolution observations of the SPHERE Integral Field Spectrograph allow to constrain the basic atmospheric properties of the planets, like the effective temperature, but it leads to significant degeneracies in the determination of additional parameters like the surface gravity, the metallicity, the composition, or the presence of clouds when fitting atmospheric models (e.g. Bonnefoy et al. 2016). The latest generation of models incorporate the best of our knowledge of cool planetary atmospheres to produce realistic synthetic emission spectra of planets. These models define the boundary conditions of the evolutionary models and are key to predict absolute magnitudes in given filter passbands (that are more accessible than bolometric luminosities). Most atmospheric models account for the formation of cloud particles of different composition (silicates, sulfites...) and sizes. Clouds are critical but complex component of the models, modifying the atmospheric structure (pressure-temperature profile), opacity, and composition (depletion of chemical elements). Each family of atmospheric models consider its own prescription of cloud physics and additional ingredients such as the non-equilibrium chemistry and the thermochemical instability are proposed to regulate the atmospheric properties.

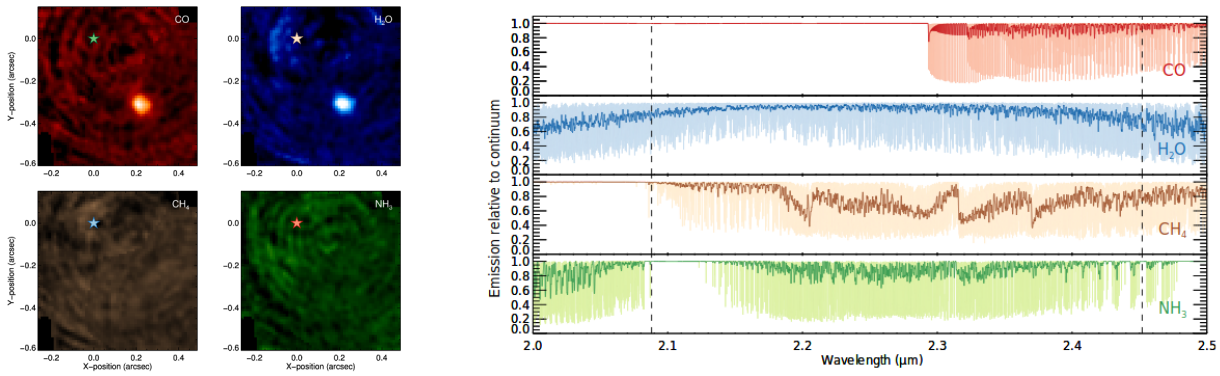

Figure 7: *Left,* VLT/SINFONI Molecule maps of CO, H2O, CH4 and NH3 at vsys=0 km/s of β Pictoris b. In all four panels, the colours scale linearly between cross-correlation values of -0.05 (black) to +0.2 (white). A cross-correlation enhancement caused by the planet is detected at a signal-to-noise ratios of 14.5 and 17.0 in the maps of CO and H2O respectively, but not in those of CH4 and NH3. *Right,* Model templates of CO, H2O, CH4 and NH3 at high spectral resolution of $R = 10^6$ (light colour) and convolved to a spectral resolution of $R = 5000$ (dark colour). The vertical dashed lines indicate the wavelength range of the data. (see Hoeijmakers et al. 2018).

To alleviate current degeneracies and fully explore the physics of atmospheric models, accessing a higher spectral resolution is vital:

- to study for instance the accretion processed at play during the formation of giant planets,
- to measure the composition and abundances of specific elements tracing the origin of formation like carbon and oxygen,
- to characterize the clouds properties (composition and size distribution) and their spatial horizontal and vertical repartition,
- and, by accessing resolutions of at least $R_\lambda = 5000$, to resolve individual molecular lines (CO, CH_4, H_2O, NH_3) to even start being sensitive to the radial velocity shift or rotational broadening induced by the planet's orbital motion or rotation (Snellen et al. 2014).
- Finally, temporal monitoring might then open the possibility to apply Doppler imaging technique, which relies on line profile variation during the object rotation period, to actually map the 3D structures and composition of the exoplanetary atmospheres as achieved for Luhman 16 B by Crossfield et al. (2014).

(2) Boosting current detection performances using atomic/molecular mapping

The intrinsic spectral features of the planets can also be used to improve the detection sensitivity. This is partly used in the spectral differential imaging technique in combination with angular differential imaging (ADI), but in fact this technique relies more in the similarity of the speckles at different wavelengths than on the spectral features of the planet, although some detection limits estimations do use spectral templates to estimate the sensitivity to different spectral types (e.g. T-LOCI, Marois et al. 2010; Ruffio et al. 2017). To really benefit from the fact that the star and planets have very different spectral features, resolutions higher than at least 1000s (ideally 10000s) are necessary. Several emblematic examples have demonstrated the interest of medium and high-resolution spectroscopy for the detection (β Pictoris b with VLT/SINFONI shown in Figure 7, PDS 70 b and c, Hoeijmakers et al. 2018; Haffert et al. 2019) or characterization (β Pictoris b with VLT/CRIRES, HR8799c with

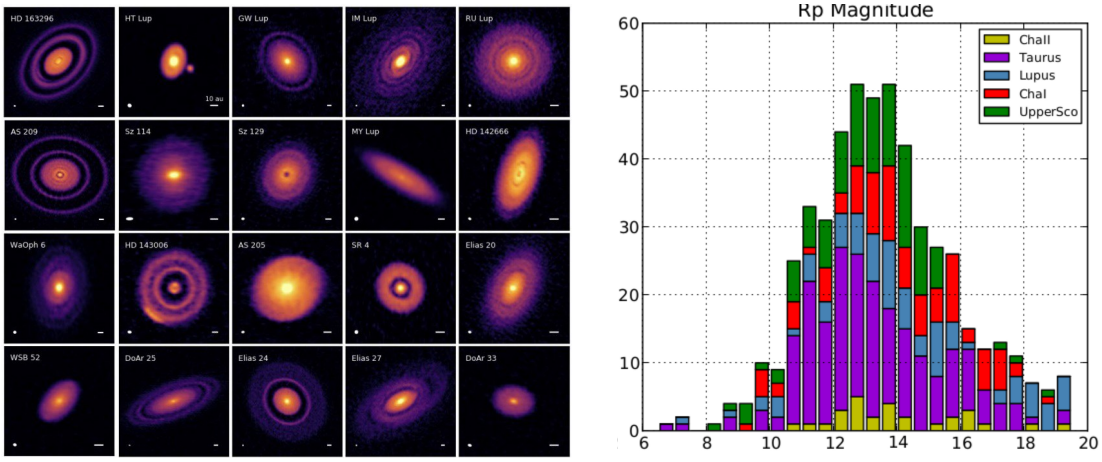

Figure 8: *Left,* DSHARP ALMA protoplanetary disk discoveries. *Right,* Histograms of young members of nearby star-forming regions, prime targets of ALMA observing campaigns including the DSHARP survey. SPHERE current cutoff of high-Strehl correction is located at $R = 9.5$. (e.g. Andrews et al. 2018).

Keck/OSIRIS, Snellen et al. 2014; Konopacky et al. 2013) of known companions. In such cases, the correlation of the extremely faint planetary signal with pre-computed spectral templates enables to significantly boost the detection sensitivity. Even in extremely noisy data dominated by stellar photon noise or detector noise, the planetary signal can be isolated and retrieved via a cross-correlation function. One of the important goals of SPHERE+ will therefore be to provide higher spectral resolution for the characterization, but also to allow further discovery of young giant exoplanets. There are several possible pathways to reach this goal, which have different levels of maturity and technical requirements, and are developed here after.

Accessing medium ($10^3 - 10^4$) to high (10^5) spectral resolution on planets discovered by SPHERE or newly detected by SPHERE+ will enable:

- to explore a new space of physical parameters for young Jupiters including a better characterization of the effective temperature, the surface gravity, the metallicity, the composition, the cloud properties, but also a direct measurement of the relative abundances tracing the origin of formation, the planet radial velocity and orbital period, to even hope acquiring Doppler images of the molecular and atomic absorption/emission lines of the exoplanetary atmospheres,
- to boost the detection performances by combining xAO high contrast performances and highly-dispersed techniques pioneering the path for future ELT instruments as HARMONI and METIS.

3.1.3 Witnessing planetary formation in action (`sci.req.2`)

With ALMA, high angular resolution observations of proto-planetary disks have revolutionized our view of disk evolution and showed that small-scale structures such as concentric rings and spiral arms are ubiquitous (e.g., Andrews et al. 2018), confirming that planet formation might occur very early in the history of a young stellar system. Although these substructures are often interpreted as direct imprints of planet disk interactions, it is still challenging to understand and constrain the architectures of planetary systems that are needed to account for them (e.g., Bae et al. 2018), or to rule out alternative scenarios (e.g., magneto-hydrodynamical instabilities, Flock et al. 2017). Today's DI surveys reach detection limits of a few Jupiter masses, but are often limited by bright and complex disk features. Numerous claims of companion candidates in disks that show asymmetric features are

indeed still debated or even rejected (e.g., HD 100546, HD 169142, MWC 758, LkCa 15). The recent discovery and confirmation of a young, dusty 7 M_{Jup} planet in the young transition disk surrounding PDS 70 using SPHERE opens the perspective for a more systematic search and characterization for young proto-planets in the highly-structured protoplanetary disks observed with ALMA (Keppler et al. 2018, 2019). Increased wavefront sensing capabilities toward faint stars (used as reference for the xAO), as proposed for SPHERE+, will lead to further discoveries of PDS 70 system analogs (and even younger ones), unique to study the physics of accretion processes and shocks leading to the formation of giant planets (see Figure 8). Connecting the proto-planet properties with the disk structures and the markers of accretion will significantly help to understand the formation of giant planets and of their atmospheres from the theoretical point of view.

Accessing fainter stars with SPHERE+ offers the perspective:

- to study the close environment of very young ($\lesssim 10$ Myr) stars from the closest and emblematic star-forming regions of Taurus, Lupus, Chamaleontis, Scorpius, marginally explored with SPHERE, and offering a strong synergy with ALMA, and the perspective to explore the physics of accretion of forming giant planets and the properties of young circumplanetary disks that will form exomoons,

- to extend the study of exoplanets around very-low mass stars down to the substellar regime, a domain marginally explored given SPHERE current capabilities.

For accretion markers, ZIMPOL has been capable of achieving unprecedented angular resolution ($\sim$20 mas) in visible. Although exoplanets are extremely faint in reflected light, young accreting planets and brown dwarfs can be observed in very narrow bands in lines tracing accretion like H_α (but also Pa_β, Br_γ in near-infrared). The huge potential of H_α investigation has been testified by recent detections of actively accreting companions with *HST* (GQ Lup b and DH Tau b, Zhou et al. 2014), Magellan/MagAO (HD 142527 B, PDS 70b, Close et al. 2014; Wagner et al. 2018), and more recently VLT/MUSE (PDS 70b, and c, Haffert et al. 2019). Observed contrasts in H_α for all these detections was of the order of 10^{-3}, which is a factor 100 shallower than the limits already achieved on-sky using fast-imaging datasets from the SHARK-VIS Forerunner (Li Causi et al. 2017).

Accessing high contrast in the H_α emission line in the visible with SPHERE+ offers the perspective:

- to provide direct clues on the mass accretion rate of the companions, as observed in low-mass young stars (e.g. Alcalá et al. 2017). An H_α survey program on nearby star-forming regions (e.g. Chamaeleon, Taurus, Lupus) can therefore provide crucial constraints on the formation mechanisms and time-scales for wide-orbit giant planets and/or close-in brown dwarfs.

3.2 Disks and planetary systems

Disk science is tightly connected to Exoplanet science as disks are the birthplace of planets. Although not driving most of the technical requirements except the field of view, disk science will directly benefit from the improvements associated to the SPHERE+ design. While the contribution of SPHERE to disk science is already impressive, there are still a lot of pending questions, which critically depend on SPHERE performances. The keywords closer, deeper, fainter, higher spectral resolution are all still meaningful in this context. These questions are many fold but could be gathered in two main categories, which we describe below. At the same time we provide how scientific requirements translate into instrumental requirements.

1) How and when planets form in protoplanetary disks and how they evolve into the debris disk phase?

Planets are expected to form in a few Myr depending on which mechanism is at play (core accretion vs. gravitational instability). Exploring the environment of young stars ($< 10 \sim 30$ Myr) is therefore necessary to understand the various stages of planetary formation. While such stars are precisely part of SHINE, so far we have 1) evidence of a direct connection between disks and planets for only a handful of systems (beta Pic, PDS 70), 2) some indirect evidences of disk hosting planets coming from multi-wavelength, multi-instruments data (HR 8799, HD 95086, 51 Eri, ...), and 3) many structures theoretically attributed to planet formation or disk-planet interactions. From these data, we already learned a lot in this field but addressing this science case in an exhaustive way simply requires increasing the statistics for a better sampling of the parameter space, which essentially is represented by system age, stellar mass, disk size and mass. It is desirable to extend these parameters towards younger (< 1 Myr) and older (> 30 Myr) ages, low mass stars (M type stars), as well as angularly smaller ($< 0.5''$) and fainter disks (contrast $> 10^{-5}/10^{-6}$) to cover the evolutionary sequence.

As mentioned before, directly imaged planets are rare but indirect signatures are very common, especially in scattered light. As of today, disks observations are more efficient for Herbig and the brightest T Tauri stars, leading to the identification of the most massive disks around the most massive stars. But are these signatures still present in disks around lower mass stars, the most common stars in the galaxy? In that respect the availability of scattered light images of various types of disks is crucial to identify potential planet-disk interactions and to perform a comparison with the structures which can be observed in other spectral range, in particular with ALMA.

Also, planets are susceptible to migration, as evidenced by the many planets found in radial velocity or transit at short orbital periods. These observations however relate to old systems, when migration is already completed. In the course of their migration, planets can open gaps which eventually will stop migration, and imaging is the only way to constrain the locations and the time frame of such gaps. A systematic mapping of gaps with respect to system age provides a way to witness migration in planetary systems. Here again, the comparison of SPHERE and ALMA images is crucial to understand how planetary evolution constrains the dust particle size distribution.

Finally, there are several systems for instance, in which the identification of planets is debated because other evidences suggest they are in fact disk sub-structures. For some directly imaged planets or candidates, several studies claim the presence of circumplanetary disks since accretion is still ongoing in the first Myr or so. Given the angular resolution, which at such distances translates into several AUs, other diagnostics are necessary to identify whether disk structures can be accretion disk or not. Investigating the morphology of the inner disk region for different grain population is therefore crucial. Grain segregation in disk gaps and cavities can tell us what is causing the morphological features.

Disk science with SPHERE benefits from a strong synergy with ALMA at sub-millimetric wavelengths, but also in a near future with JWST in the mid-IR (despite a degraded spatila resolution). In that respect multi-wavelength observations are crucial to better characterize the spatial distribution of the dust, each spectral range being sensitive to different typical grain sizes. SPHERE measures pure scattered light, while ALMA is sensitive to thermal emission, and JWST can detect a mix of both. For all science cases discussed in this section, morphological and photometric studies from near IR to sub-mm will be valuable but requires to be able to observe the very same systems (in particular with SPHERE and ALMA, Fig. 8). Extending the observations of SPHERE towards lower mass stars in Taurus, Aurigae, Lupus, or Chamaeleontis associations with much better performances than currently is what we aim for. Increasing the number of disk observations around more stars to probe the parameter space and to carry out the science described here above requires:

- observing a larger sample of younger stars: such stars lies in more distant associations (>100pc), hence guide stars can be too faint and the extinction in the visible too large. Therefore,

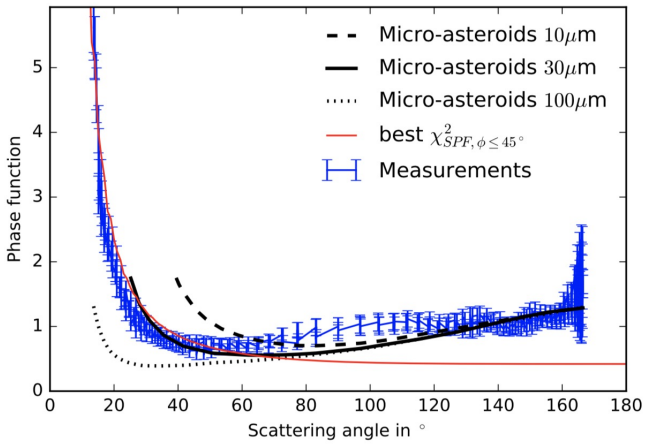

Figure 9: Scattering phase function of the debris disk HR4796 (Milli et al. 2017) compared to models of grains with various sizes showing how important are the small scattering angles to constrain the grain size distribution.

SPHERE+ should be able to increase the sensitivity to redder stars. The wavefront sensor of SPHERE is already a very performant camera (but limited to R<13.5-14 with a fast decrease of performance beyond R=10-12), hence wavefront sensing should be performed in the IR.

- observing fainter disks and fainter structures: at larger distances and/or for older systems, disks will be more difficult to detect. Increasing the polarimetric efficiency of SPHERE as well as the polarimetric precision is the key to reveal such faint objects.

- observing smaller disks: disk size will obviously scales linearly with the distance to the observer, so disks are typically smaller than 1" or so when more distant than ∼100pc. Observing smaller disks, or closer-in regions of the nearest stars where planets do form, requires to achieve higher contrasts close to the optical axis and as close as what is allowed by the coronagraphic mask.

- Achieving the maximum possible resolution allowed by VLT in the visible (∼15 mas, that is ∼2 au at the distance of the nearest star forming regions) will allow to have details of the accretion process on forming giant planets. At a typical separation of ∼200 mas (that is at ∼30 au from the star) this corresponds to resolve the Hill sphere of a Jupiter mass planet. This allows to study how gas flows from the disk towards the planet: this is expected to occur through spiral arms (Machida et al. 2010). Tantalizing evidence for this has been observed with SPHERE in the case of the proposed planet around HD 169142 (Gratton et al. 2019b) and with SINFONI for PDS 70b (Christiaens et al. 2019).

2) What are the dust properties along the evolutionary sequence?

As the gas dissipates, dust grains settle in the midplane and grow. This component is incorporated into planet cores and planet atmospheres. Later, the dust observed in debris disks is resulting from collisions between planetesimals hence can have different properties. Investigating the variation of dust shape, size distribution and mineralogy as a function of stellar mass, and system age is key for understanding planet formation or planet environment. SPHERE has two means to characterize such properties, either from polarimetry or from photometry/spectroscopy or both.

When these techniques are combined, the scattering phase function can be extracted either in polarized or unpolarized light, possibly at different wavelengths, to reveal the composition, shape and size of the grains. This requires a comparative measurement of polarized and unpolarized signals.

However, the data processing that we are using for non-polarimetric disk images involves the technique of angular differential imaging, which strongly affects disk signal with self-subtraction. In contrary to point-sources (planet image), the disk intensity can only be partly recovered with forward modeling. But, this is not sufficient for a thorough analysis of grain properties. To overcome this limitation, we need to generalize the technique of Reference Differential Imaging, which historically was the first to be used on ground-based telescopes, but reached its optimal interest with HST. This is crucial for disk science and calls for a very stable and homogeneous performance regarding the xAO system.

Resolved photometry or spectroscopy (meaning we have information at several phase angles) has been performed in a very few cases (Milli et al. 2017, 2019, Bhowmik et al, in prep.) and already provides crucial elements about size distribution either by measuring the scattering phase function (Fig. 9) or the spectrum. The canonical picture of debris disks presumably populated with grains of size larger than the blow out size is starting to evolve. Particle shapes appear more complex than compact spheres, with phase functions suggestive of large and porous aggregates, consistent with in-situ measurements of solar system comets, and informing us on the conditions of dust growths in the very first stages of planet formation. In addition, several ALMA observations provided evidence of gas (possibly from 2nd generation) in debris disks, which modifies the dynamical behaviour of grains.

Mineralogy is obviously an important aspect too, but such level of characterization favour large spectral coverage hence the need to combine several instruments (SPHERE, JWST). Again, this aspect is pointing to the capability of observing the very same objects with various facilities.

Finally, the inner regions where warm dust is co-located with planets (even terrestrial) has been little explored in both protoplanetary and debris disks. This region is of interest to understand how and when dust dissipates from the inner system and to connect interferometric observations of exozodii with direct imaging. Given the increase of scattered light as the square of the stellocentric distance we can expect these regions to be rather bright.

The requirements expressed in the previous case still hold for this second science case but can be further developed as below:

- exploring the warm dust content located at <5 au requires to push the contrast limit at 2-3 times shorter separations.
- measuring the disk surface brightness (total or polarized) at the smallest scattering angles: this can bring strong constraints about grain sizes but requires to achieve larger and more stable contrasts with no or little impact coming from the data reduction (so called self-subtraction in angular differential imaging).
- measuring disk surface brightness with spectroscopy: SPHERE IFS provides a very low resolution (30-50) which is sufficient to measure spectral slope (grain size dependent) but not sufficient to identify spectral features, if any are present. Therefore, higher spectral resolution (required for planet searches) would be beneficial to better study mineralogy.
- Combining polarimetry and spectroscopy: SPHERE currently is able to perform polarimetry in broad-band. The potential of combining both spectral and polarimetric information even at low resolution is relevant for thorough characterization of grain properties at different stages of the evolutionary sequence.

3.3 International context

3.3.1 Positions with respect to other high-contrast imagers on 8m to 10m-class telescopes

High contrast imaging has been an intense subject of development in the last decade. The availability of 10-m class telescopes was decisive for this field as the corresponding angular resolution achieved

in the near infrared with AO started to be suitable for being sensitive to planetary system scales. As a result, most of the 10-m class telescopes were or are about to be equipped with xAO coronagraphic instruments, like:

- the Gemini Planet Imager (GPI, Macintosh et al. 2014) being one of the main competitor to SPHERE. The strength of SPHERE in this landscape mostly relies in the: i/ the number of modes serving several science cases, ii/ the large field of view, iii/ the global stability, iv/ the snapshot observations of a large spectral range, and v/ the large amount of GTO nights. GPI is now being decommissionned and is planning for an upgrade (GPI 2.0) before being re-installed at Gemini North. GPI 2.0 (Macintosh et al. 2018) should include an upgraded xAO as planned for SPHERE+ (faster correction, better sensitivity), but will not provide higher spectral resolution, which provides SPHERE+ with a significant advantage.

- the Subaru Coronagraphic Extreme Adaptive Optics (SCExAO) instrument is a modular high-contrast instrument installed on the Subaru telescope in Hawaii. SCExAO benefits from a first stage of wavefront correction with the facility adaptive optics AO188, then forms an image on the 2000-actuator deformable mirror (DM) linked to a Pyramid WFS camera to provide with a second-stage AO an xAO correction in the near-infrared. SCExAO then feeds the integral field spectrograph CHARIS, with its J, H or K-band high-resolution mode or its broadband low-resolution mode, or the new Microwave Kinetic Inductance Detectors (MKIDs) Exoplanet Camera (MEC).

- the Keck Planet Imager and Characterizer (KPIC) project (Mawet et al. 2018). KPIC consists of an insertable/removable module downstream from the current Keck AO system, equipped with its own efficient infrared wavefront sensor (IR WFS) using the latest low-noise detector technologies (IR-APD), a high-order deformable mirror(HODM), a state-of-the-art coronagraphic bench, and a steerable beamsplitter dividing the science beam into an imaging path and a fiber-injection unit. Both channels are available to feed existing infrared science instruments available at Keck: imager (NIRC2), IFU (OSIRIS, or another IFU yet to come) for the imaging channel, and high resolution spectrograph (NIRSPEC) for the fiber-fed spectroscopic channel. In that sense, KPIC presents a very similar and competitive upgrade compared to SPHERE+.

- Finally, at VLT, we can highlight the strong synergy of SPHERE+ with the ERIS instrument at UT4 (Davies et al. 2018). ERIS, that will be commissionned in summer 2020, is a near-infrared AO-fed spectrograph which will exploit the exquisite correction of the AOF on UT4. It will replace the SINFONI medium resolution spectrograph and the thermal infrared high-contrast imaging mode of NaCo. Some ERIS observing modes are tailored for disk and exoplanet direct imaging, but restrained to the thermal infrared domain at L and M bands. These are clearly favorable bandpasses for taking advantage of a reduced star/planet contrast, but in broad band. In addition, wavefront sensing is performed in the visible which restrains the sample to bright targets and limits the sky coverage. In that respect, SPHERE+ will provide spectral characterization of planets and disks at shorter angular separations with higher angular resolution, and is therefore very complementary to ERIS, and to a larger extent with ALMA for a global characterization of young planetary systems.

In summary, in this extremely competitive instrumental and scientific field, SPHERE+ will bring a significant evolution of the current SPHERE instrument to perform cutting-edge science. It will provide ESO with the most performant, most effective, planet imager in the southern hemisphere for the next decade so that the VLT can maintain a world-leading position in the field of direct imaging of disks and exoplanets for the upcoming decade, and to ensure a smooth transition towards even more ambitious facilities on the ELT.

3.3.2 Positions with respect to ELT

On top of the science perspectives enabled with SPHERE+ as described here above, the development and operation of such a new facility at the VLT is also an important step towards the science and the instrumentation envisaged for the ELT.

Regarding the scientific synergy with the ELT, the SPHERE+ instrument at VLT will remain a dedicated planetary imager designed to survey a large number of targets including: i/ young, nearby stars previously observed with SPHERE owing to the enhanced contrast capabilities offered by SPHERE+ to explore physical separations below 10 au, ii/ new promising systems identified by *Gaia* and ongoing/forthcoming RV studies (HARPS, NIRPS, Spirou, ESPRESSO...), and iii/ faint members of more distant star-forming regions well studied with ALMA but currently out of reach of the current generation of xAO planet imagers. SPHERE+ at VLT will therefore pave the way for the ELT instruments to identify the most interesting systems for dedicated ELT observations focused on the characterization of these systems and to search for additional lighter planets. Given the expected community pressure on the ELT, preparatory survey as proposed with SPHERE+ at VLT will ensure an optimal use of the ELT observing time.

Regarding the instrumental synergy with the ELT, in the perspective of 1st light instruments, the proposed new adaptive optics module for SPHERE+ will include a similar type of sensor (Pyramid wavefront sensor) as the MICADO, HARMONI and METIS SCAO systems. The pyramid sensor concept was proposed quite a while ago and a few systems are in operations but we know that, on top of the theoretical principles, a crucial key to success for an operational system at full performance is also the actual know-how of the development and integration team. HARMONI, MICADO, and METIS SCAO system designs are already well advanced, have passed PDR, but the SPHERE+ project would provide feedback from earlier in-lab critical tests of a full closed-loop and also on-sky operational experience. The high contrast goal of SPHERE+ also enforces the need to fully understand the quality of AO measurements at a high level of accuracy. While ELT SCAO systems are expected to deliver a lower image quality than SPHERE+, they can be as demanding in terms of the number of AO measurements given the much larger pupil size. The AO community in Europe has a long background and practical actions to organize and share expertise. This can be seen for instance currently in exchanges and active collaborations on Pyramid wavefront sensors, control laws, search for synergies on LGS WFS between HARMONI and MAORY,... The SPHERE+ effort would fit within this search of synergy between institutes and connecting to the development of ELT instruments.

On a longer term, achieving spectroscopy of mature telluric planets remains one of the most appealing driver for a high contrast imaging facility on the ELT. The METIS instrument and its combination of high-angular resolution and high-spectral resolution integral field spectroscopy in thermal infrared will represent another step towards this goal. A full exploitation of the ELT capabilities will then arrive with the Planetary Camera and Spectrograph (PCS). PCS requires a mature concept to solve the technical challenges which were identified during the EPICS phase A study. The roadmap towards this prime objective will be supported by new developments concerning critical components (including detectors, deformable mirrors, ...) but not only. It also requires timely tests and demonstration of new functionalities and concepts, on-sky. The proposed SPHERE+ project includes a number of new major ideas (AO concept as well as medium/high resolution spectroscopy) which will open the way for a convincing, possibly alternative, PCS concept. Exploring the full potential of these novel ideals, as it is mandatory to address the most ambitious goals of PCS, requires the actual on-sky experiment in good conditions that SPHERE+ can provide. In this context of preparing an ambitious 2^{nd} generation ELT instrument the development of SPHERE+ is timely to provide feed-back in the mid 20's.

4 Technical requirements

To address the science cases described in Section 3 we propose a series of upgrades, referring to the SPHERE+ project. The main technical requirements are 1) to achieve higher contrasts at shorter separations, 2) to increase the sensitivity towards red targets, and 3) to perform better atmosphere characterization with medium to high spectral resolution. At this stage, and after a 1-year phase of brainstorming, we already made important design choices in anticipation for a phase A. Improvement of the contrast close to the optical axis is brought primarily with a 2nd-stage xAO system (SAXO2) combined to a pyramid IR wavefront sensor, altogether allowing faster correction (`tech.req.1`) and more sensitivity to red targets (`tech.req.2`). Further improvement of contrast at short angular separations is provided by a combination of optimized coronagraphs, and algorithms for compensating non common path aberrations. Some polarimetric components are refurbished or modified to improve efficiency. SPHERE+ also aims for a full exploitation of the spectral dimension in high contrast imaging, essentially by providing higher spectral resolution that what is currently possible, either in a narrow field with medium resolution, or in a single location of the field but at high resolution (`tech.req.3`). Since the xAO proposed solution does not benefit to the visible channel of SPHERE we also consider a fast visible camera to tackle a very particular but appealing science case. The following sections describe the crucial ingredients of the SPHERE+ concept.

Describe preliminary concept and objective of the phase A:
- WFS (pyr + detector)
- DM
- RTC
- interfaces

4.1 Extreme AO

4.1.1 SAXO2 main requirements

The science goals push for a better contrast at small separations especially within $0.3''$, achievable on a remaining large target sample: early-type stars will be probed up to > 100 pc which correspond to still bright targets, but lower mass stars or reddened young objects are also of primary interest, corresponding to red and fainter targets up to $J \lesssim 14$ considering a typical ($R - J = 2$ mag) color for ALMA targets in young star-forming regions shown in Figure 8.

The distribution of this goal over the various instrument parts emphasizes the role of the AO turbulence correction to an even better level than current SPHERE. It does directly reduce the coronagraphic stellar halo (aka image "raw contrast") which drives the corresponding fundamental limit of photon noise (the photon noise will be dominant and driving the total integration time in the case of high resolution spectroscopy characterization, Sect. 4.4.2, and medium-resolution IFU detections, Sect. 4.4.1). It also makes possible the integration of new coronagraphs (sec. 4.3) with smaller Inner Working Angle for detection at separations less than 250 mas. Finally it also makes more efficient and performing the measurement and compensation of static or slowly evolving Non Common Path Aberrations driving the speckle noise limit.

More specifically, the main requirements for AO improvement are:

- a better correction of moderately low order modes (`tech.req.1`). It primarily requires a faster effective correction; it also requires a better control of aliasing effects (preventing uncorrected high modes to fold incoherent light back to short separations).
- improved AO sensitivity, especially for red stars (`tech.req.2`).

The following describes the various components of saxo2

4.1.2 Performance gain within reach with available technology and expertise

The choice of a *Pyramid wavefront sensor* (P-WFS) is the obvious and ideal option here to answer the previous requirements. Thanks to well-understood noise propagation properties, this sensor is intrinsically more sensitive than the current Shack-Hartman sensor, and shows better anti-aliasing properties

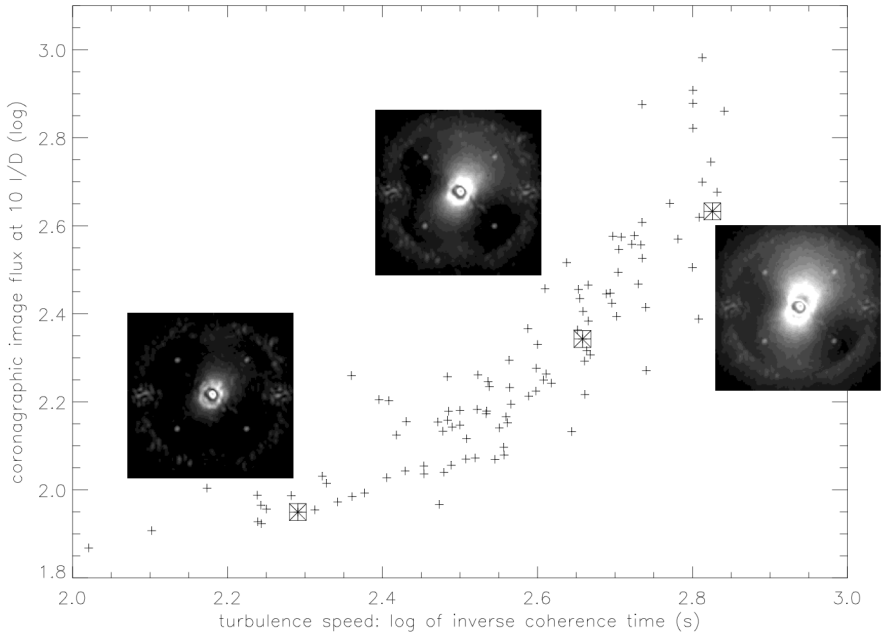

Figure 10: Correlation between the coronagraphic image raw contrast at 10 λ/D and the turbulence speed (inverse coherent time in log scale: slow turbulence on the left, faster towards right). Inset images correspond to the squared data points sampling the halo intensity in three different cases from slow, medium and fast turbulence. These data are extracted from a single long observing sequence (constant instrumental setup) in H band on a bright target. The comparison between the left and right image insets are indicative of the impact of the change by a factor 3 of the turbulence speed (for a given AO correction bandwidth). In other words, the proposed upgrade will routinely change the right image (currently obtained in most conditions) into the left image (currently obtained only the rare slowest turbulence conditions)

can measure the low wind
pyramide non modulé

and small tip-tilt residuals. Moreover, it requires fewer detector pixels. This makes possible the use of fast and low-noise detectors already commercially available for both visible and NIR domains[3]. These good properties were also the reason for its selection for the ELT-SCAO. This induces here an important synergy as mentioned in Section 3.3.2: lab experiments are actually currently at work in preparation to such ELT projects, developing and consolidating the same necessary expertise on such sensors, and SPHERE+ could not only benefit from them, but also provide earlier on-sky feed-back of the measurement and correction of a similar number of degrees of freedom, in easier conditions than the 1st ELT instruments commissioning.

The concept is mature and in synergy with ELT. The critical components are also directly available. In particular, some low-noise NIR (from 800 nm) or visible camera can be procured with the appropriate format and with a frame rate up to more than 3 kHz, i.e. close to 3 times faster than the current SPHERE loop. From this basis, we have a very good support to predict the corresponding *contrast gain*: the analytical model of AO correction predicts the gain in residual wavefront errors close to the axis where the lag error dominates, and this prediction is actually well verified on SPHERE data (see Fig 10, extracted from Mouillet et al. 2018). On the SPHERE coronagraphic images, the residual WFE errors are translated into stellar halo intensity, limiting the raw contrast. On-sky SPHERE data actually demonstrate such expectations on how the raw contrast is improved with a better AO correction bandwidth over turbulence timescale $I \propto (AO_{speed}/turbulence_{speed})^{1.5\sim2}$. Looking at the performance currently obtained in the rare observing cases of slow ($\tau_0 > 6$ ms) turbulence tell us about what will be obtained routinely with a 3 times faster SPHERE+ (`tech.req.1`). The corre-

[3]Note that four SELEX SAPHIRA detectors have already been in operation on Paranal since 2016 in the four GRAVITY CIAO wavefront sensors

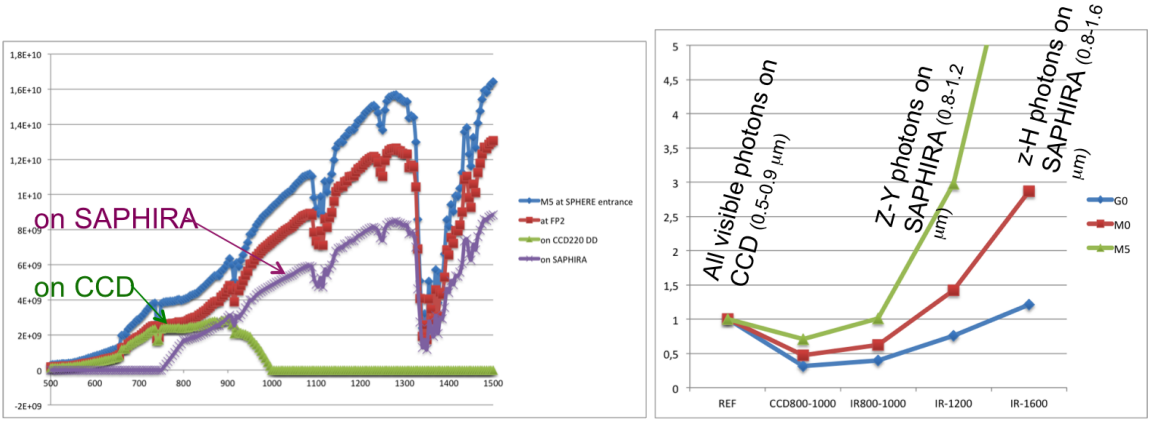

Figure 11: Photon rate on WFS sensor: comparison between sensing in NIR and VIS. Left: photon rate obtained from a M5 star as a funcxtion of wavelength as arriving at the entrance of the system (blue curve), after the common-path reflective optics up to the intermediate corrected focus (red curve) and finally detectable according to the detector quantuum efficiency onto either a visible CCD (green curve) or a NIR SAPHIRA-type detector (purple curve). Right: Comparison of the amount of collected photons with respect to the current case when observing in NIR where all the visible photons are used by the WFS. The comparison is made for different assumptions of photon-share and different stellar types: G0 (blue), M0 (red) and M5 (green).

sponding raw contrast gain by a factor 5 to 10 is a minimum value that could even be improved thanks to better control laws (see below).

Associated to this ready-to-be implemented faster loop, the *sensor sensitivity* is important to benefit from this improvement on a large target sample, and even to address fainter stars with the current correction level (`tech.req.2`). We already mentioned that P-WFS is intrinsically more sensitive than the SH-WFS (pushing the limiting magnitude to typically 15 mag). Reconsidering the design here, we propose also to shift the sensing spectral domain to the red-NIR part. For instance, a M0 star (resp. M5 star, such as the proto-type Prox Cen) would provide 1.5 (resp 3 !) times more photons within the 800-1200 nm spectral range than in the current 500-900 sensor range (when accounting for the stellar spectrum, but also the instrument and detector efficiency, Fig. 11). The gain for a M0 star is even up to a factor 3 when considering the 800-1600 nm range: such a comfortable advantage opens up the possibility to discuss various grey photon share optimizations between the sensing channel and the science instruments.

4.1.3 Implementation scheme minimizing interfaces, AIT and system risk

in the management

If the expected performance improvement is securely motivating, based on current expertise and available components, we consider also *the implementation options*, and discuss the testing phase, including the estimated time needed on telescope and the corresponding risk. The approach we propose significantly minimizes these two aspects by providing such a faster correction as a second correction stage, after and essentially independent from the existing one. The current SAXO system (and all its operating interface with the VLT, de-rotator modes, calibration scheme) remain unmodified, which guarantee no risk to degrade the current performance in all modes. On the NIR arm, after the NIR-ADC devices and before the coronagraphic plane, the beam is to be picked up to this new 2nd stage correction module. Such a module includes consistently an additional DM, and NIR P-WFS loop, working in already good conditions as provided by SPHERE SAXO and CPI, and focusing on exquisite and fast correction of the remaining low amplitude and fast residuals. Possible resonances

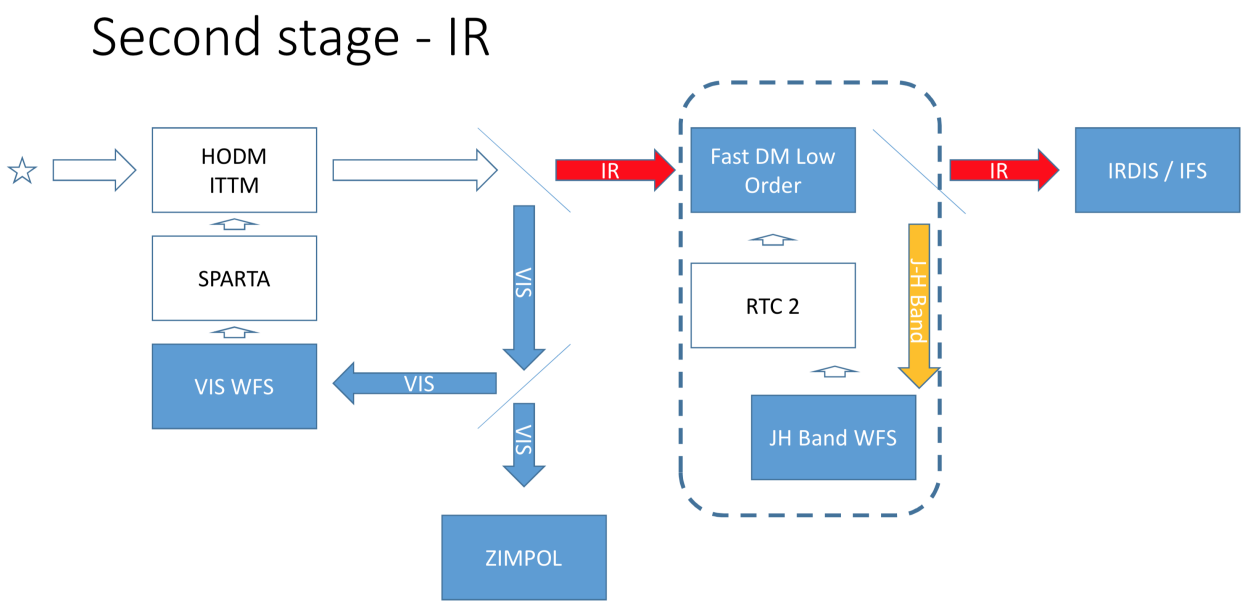

Figure 12: Schematic of the 2nd stage AO correction module, on the NIR path. The additional correction module has minimum interface with the existing and unmodified SAXO module ; it can be tested in a stand-alone AIT set-up before in-SPHERE integration. The new sensor bandpass (z-Y ; z-J ; z-H) is to be optimized according to science cases with sensitivity gains of a factor 5 to 10 depending on the stellar spectral type.

between SAXO1 and SAXO2 should be investigated in phase A. This module is essentially self-consistent with the advantage of the possibility to test it intensively in Europe before integration, and few operating interfaces.

Because the priority is set here to minimize interfaces, implementation time and risk, this new module feeds only the SPHERE NIR arm and does not impact the visible arm (feeding ZIMPOL). Science in visible could also benefit from better contrast and sensitivity: it is proposed to consider such a possibility in a later stage, in a potentially simpler and less risky manner than trying to cope both purposes at the same time now. At that time, options could be to duplicate this module on the visible arm, or to use this module sensor to control the main loop with better performance (but this would probably not be cheaper and surely more complex). An alternative for improving performance in the visible could also relies on a better exploitation of the speckle field statistics as discussed in Section 4.6. A safe decision could be better made on the basis of the SPHERE+ achievements.

4.1.4 Keeping SPHERE at performance edge towards future ELT planet imager

On top of the robust and strong advantages in terms of raw contrast performance in the NIR of this new AO module, based on secured models and available components, we also identify some important margins for additional performance improvements. First, this additional correction stage is the ideal location to implement new predictive control algorithms. Theoretical and simulation works have already demonstrated the potential of this approach, especially in good correction regime, to enhance the correction bandpass. The actual implementation in good conditions requires a stable and well-understood AO platform which is exactly provided by SPHERE. Here again, this development could be fully developed and tested in lab before its use and benefit on telescope. Second, an accurate and fast sensor in the same spectral bandpass and close to the coronagraphic plane is also very important to minimize all chromatic or variable differential aberrations which are not yet the dominating limitation to ultimate contrast but which is the next challenge to tackle just after the better turbulence correction.

Figure 13: Comparison of an AO-corrected coronagraphic image with the current SPHERE AO design (left) to the proposed additional 2nd faster correction stage (right). Typically 10 times deeper raw contrast is obtained at short separation, up to a radius depending on the 2nd DM number of actuators (24×24 in this example).

4.1.5 SAXO2 summary before a Phase-A study

In summary, this general approach proposes considerable performance improvements in line with the scientific priorities, minimizing the risk in terms of expected development, expected performances, and integration phase. If agreed, a phase-A study would in particular precise the optimal photon-share options between sensor and science, precise the interfaces (in particular for opto-mechanics with SPHERE/CPI) and propose a general design and development plan for this module, in synergy with current ELT-SCAO developments. The cost estimates obviously depend on the selected design choices. Main parts include i/ the WFS path (fast low-noise detector + opto-mechanics), ii/ an additional DM (with a priority on response speed, but moderate requirement on the number of actuators, typical 20×20 or 30×30, and a small stroke), iii/ the RTC development shows no fundamental difficulty concerning the data flow and required computing power, and its complexity is significantly reduced by minimized interfaces (unlike the main SAXO loop intimately interacting with the VLT and the whole operating scheme) and the manpower directly depends on the exact interfaces and standards to be discussed with ESO, and iv/ finally the tools and testing set-up in Europe for a reliable AIT phase in Europe to guarantee an efficient and short integration time at Paranal. Figure 12 provides a scheme of the SAXO2 concept and Figure 13 display a simulation of performance with a 2nd stage which is able to get deeper at shorter separation.

Because this module is not interlaced with the current SAXO correction loop, its selection is independent from the analysis of the current high order DM in operations. This HODM (developed on a shared-risk basis with CILAS company with European support) showed a handful of dead actuators within the active pupil and some actuators with slower response time than specified. These problems appeared essentially during the test phase in Grenoble (under temperature and humidity conditions which were variable and quite different from those in Paranal). Because this component is critical for the performance, and its procurement is long, severe operational caution procedure have been defined and applied (strong humidity restriction, dry N_2 flow, monitoring procedures) at Paranal. In addition, a plan for preventive procurement of a new DM had been started, and recommendation was made by STC that long term operations should include the replacement of this HODM. Since then, in stable conditions and under this operating frame, no evolution has been detected, and the proposed SPHERE+ proposal has no impact on the way to use this DM (in particular, it will not be operated at a faster rate; its speed could actually be relaxed). As a consequence, the proposed 2nd stage has no direct relation with the decision to replace or not the current DM. Such decision on a risk mitigation basis can be made separately.

quasi stat speckles

4.2 Non-common path aberrations

Even in good observing conditions, coronagraphs produce images in which the contrast level can be degraded by many effects such as residual jitter of a few milliarseconds (mas), low-order aberrations (tip, tilt and defocus), the low-wind effect (Sauvage et al. 2016), or the wind-driven halo (Cantalloube et al. 2018). To be more general, the current limitation of contrast in the SPHERE science images are averaged speckles creating a halo (due to wavefront errors evolving faster than the exposure time: wind effects, etc), static (longer than the sequence of observations) and quasi-static (longer than the exposure time but shorter than the sequence of observations) speckles induced by wavefront aberrations mainly upstream from the focal plane coronagraph mask and, diffraction pattern.

The halo signature is very different from an exoplanet image. It does not prevent the detection of an exoplanet but it decreases its signal-to-noise ratio by adding photon noise. The only way to minimize this halo is to use a faster AO system to convert the fast-evolving aberrations into quasi-static aberrations. Static speckles can be calibrated a posteriori using observing strategies and post-processing techniques such as angular differential imaging (ADI, Marois et al. 2006) or spectral differential imaging (SDI, Racine et al. 1999). As for the quasi-static speckles, various strategies have have been investigated to stabilize, measure, and correct for them (e.g. Baudoz et al. 2010; Singh et al. 2015; Huby et al. 2015, 2017; Lamb et al. 2017; Milli et al. 2018; N'Diaye et al. 2018; Wilby et al. 2018). In the absence of or after compensation for the static and quasi-static aberrations, there is still the diffraction pattern due to spiders, central obscuration and coronagraph design. This signature is known by design.

Quasi-static speckles originate from the wavefront errors that are invisible to the ExAO system, the so-called non common path aberrations (NCPA). Anticipated at the time of designing the instruments (e.g. Fusco et al. 2006), these wavefront errors are due to the differential optical path between the ExAO visible wavefront sensing and the NIR science camera arms. On the order of a few tens of nanometers, these aberrations slowly evolve with time, producing speckles with a quasi-static behavior that makes their calibration challenging for exoplanet imaging (Martinez et al. 2012, 2013; Milli et al. 2016). In addition to post-processing techniques, this issue is currently being addressed thanks to the exploration of several solutions including online software (e.g. Savransky et al. 2012; Martinache et al. 2014; Bottom et al. 2017) and hardware (e.g. Galicher et al. 2010; Martinache 2013; Martinache et al. 2016; Wilby et al. 2017).

On SPHERE, two methods have been probed to correct for the NCPA: a Zernike wavefront sensing path called ZELDA (N'Diaye et al. 2013, 2016) and the coronagraphic phase diversity called COFFEE (Paul et al. 2013, 2014). In 2019 the pair-wise/electric field conjugation (PW/EFC) technique has also started to be studied to correct for the NCPA, and minimizes the diffraction pattern in a given focal plane area simultaneously. The current status of the ZELDA and PW/EFC tests are summarized in Sections 4.2.1 and 4.2.2 respectively.

For SPHERE+, NCPA calibration and compensation will be a key ingredient to increase the raw, and therefore post-processed, contrast in the data. There is no frozen solution. One solution combines pupil-based measurements like ZELDA and focal plane-based measurements like COFFEE or PW/EFC. This phase A study will be performed in close proximity with the study on coronagraph designs, which is the component that will directly benefit from any improvement on the NCPA.

4.2.1 ZELDA

ZELDA (Zernike sensor for Extremely Low level Differential Aberrations) is a phase contrast-based wavefront sensor proposed by N'Diaye et al. (2013) as a device that is dedicated to measuring the NCPA in high-contrast imaging instruments, either space- or ground-based application. Pupil images obtained with and without the focal-plane phase mask are used to reconstruct optical path difference (OPD) maps that represents the wavefront for every pixel in the pupil. In SPHERE, a ZELDA prototype optimized to work with the IRDIS `FeII` narrow-band filter ($\lambda = 1.642$ μm) was inserted into

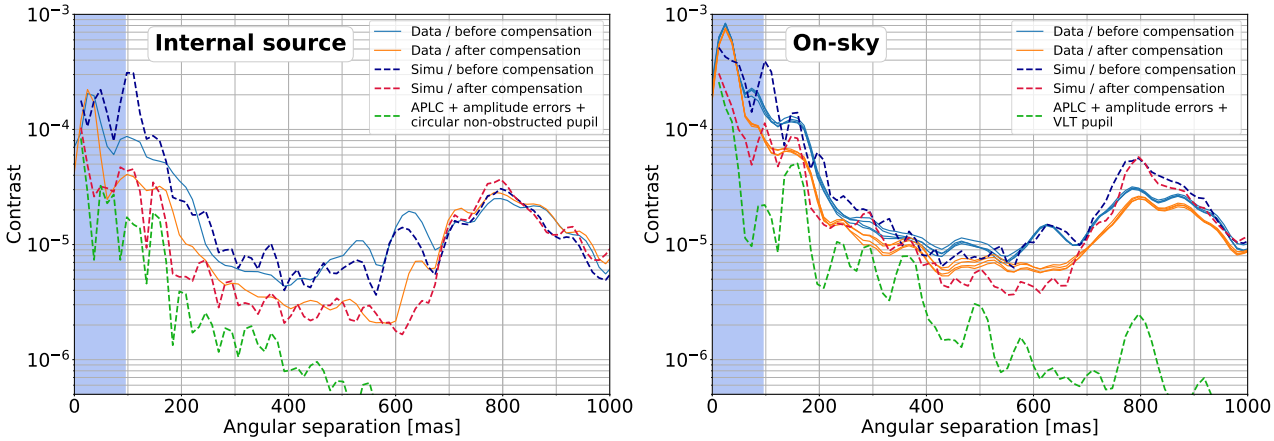

Figure 14: Coronagraphic profiles acquired with SPHERE on 2018-04-01 on the internal source (left) and on sky (right), before and after compensation of the NCPA measured with ZELDA (Vigan et al. submitted). The plots also include profiles resulting from simulations based on realistic inputs that match very closely the experimental data. The theoretical performance of the current APLC in presence of amplitude errors is also plotted (dashed green curve). The blue shadowed region shows the region masked by the focal-plane mask of the APLC.

the infrared coronagraphic wheel of SPHERE during the reintegration in Paranal.

Several tests campaigns with ZELDA were performance in 2015 (N'Diaye et al. 2016), 2017 and 2018, resulting in a demonstration that ZELDA is able to measure and compensate for the typical $\sim$55 nm rms of residual NCPA after the daily SPHERE calibrations. The 2015 and 2017 tests were all performed on the internal source of the instrument and demonstrated a gain in raw contrast of a factor 5 to 10 in the $200 - 300$ mas range.

For monitoring, we implemented in 2017 a calibration template that performs an internal closed-loop compensation of the NCPA using ZELDA. This template has been run almost daily since mid-2017, providing insightful information on the stability of the NCPA inside the instrument (Vigan et al. in prep.). Long temporal sequences of ZELDA measurements (every seconds for several hours) also demonstrated the existence of low-spatial frequency internal turbulence inside of the SPHERE enclosure, at the level of $3 - 5$ nm rms with a typical timescale of a few seconds.

The latest developments with ZELDA consisted in a validation of the NCPA compensation on-sky in April 2018 (Vigan et al. submitted). These were obtained in technical time acquired through a technical time request to ESO. These tests enabled to demonstrate that the ZELDA loop can be closed on sky. Coronagraphic tests without and with NCPA compensation allowed demonstrating that once the NCPA are compensated (either on the internal source or on sky) the raw contrast at separations below $300 - 400$ mas is limited by the design of the APLC currently implemented in the system. These results are illustrated in Fig. 14, which shows the comparison of the raw contrast obtained from the data and from the simulation model of the instrument. The main conclusions that can be drawn from these tests is that 1/ a gain in raw contrast can be obtained with a proper compensation of the NCPA (either with ZELDA or any other means), and 2/ a coronagraph offering a better contrast at very small angular separations is essential to really benefit from the NCPA minimization in the pupil plane upstream from the coronagraph.

From the operational point -of -view there are still important aspects that should be explored for ZELDA in SPHERE+. The main one is how to implement NCPA compensation with ZELDA in the operational model of SPHERE. We know that on-sky measurements and compensation show a visible improvement, however this procedure uses valuable on-sky time. It would be essential to explore the possibility to perform the calibration on the internal source and use this correction on sky. First attempts in this direction were made in 2017 but the first results were unsuccessful. Other tests are scheduled to understand the current limitation.

For SPHERE+, a more ambitious plan could be the implementation of ZELDA "on-line", i.e. running a ZELDA loop in parallel of the other AO loops in order to minimize aberrations during the science observations. This would require the implementation of a new ZELDA that can be used in parallel with a coronagraph similar to the current implementation of the differential tip-tilt sensor (DTTS) that stabilizes the tip-tilt at the level of the coronagraph focal-plane mask. Another possibility is the association of ZELDA and a control algorithm like electric field conjugation to remove the diffraction pattern in a given region of the science image (see section 4.2.2).

4.2.2 Pair-wise and electric field conjugation

The pair-wise (PW, Give'On et al. 2007) technique enables the estimation of the complex electric field of the stellar speckles that limit the contrast level in the science images. This focal plane wavefront sensor temporally modulates the speckle intensity adding known probing phases with the DM. It is then possible to retrieve the speckle electric field assuming a model of light propagation in the instrument. As the measurement uses only science coronagraphic images with no change of the instrument configuration, the estimation is NCPA-free. The remaining sources of errors come from uncertainties on the probing phases, or on the model of light propagation. The former is very small because the DM behavior (linearity, influence function, etc) is very well known in high contrast instruments like SPHERE. The latter can be minimized using all the empirical information recorded since the instrument was commissioned, as was done for ZELDA. Once the field is measured, one can use a control algorithm such as the electric field conjugation (EFC, Bordé & Traub 2006; Give'On et al. 2007) to minimize the speckle intensity in a given region of the science image that is called the dark-hole.

Laboratory performance of the PW/EFC association were demonstrated in space-like conditions reaching 6×10^{-10} contrast level at $4\lambda/D$ (Lawson et al. 2013). On a ground-based telescope, several parameters can limit the performance as demonstrated by Matthews et al. (2017).

However, PW/EFC features two main advantages as compared to wavefront sensing in a pupil plane. First, PW provides an NCPA-free estimation of the speckle electric field direclty in the science image which is the plane of interest for high contrast imaging. Then, EFC can minimize the wavefront aberrations to provide science images similar to other techniques like the current ZELDA. Doing so, the science image is dominated by the stellar diffraction pattern (spiders, obscuration, coronagraph signatures). From there, EFC can be used to minimize the stellar intensity in a given area of the science image (instead of the wavefront aberrations in a pupil plane). Such a correction results in a better contrast in half of the field for view (half dark hole) as showed in the simulated images in Fig. 15.

In this area, the diffraction pattern is decreased by a factor of ~ 2 at ~ 100 mas from the star if we assume the measurement is performed on-sky (so with the atmospheric turbulence as corrected from SAXO). This preliminary result from numerical simulation is encouraging and we will request technical time to test PW/EFC on SPHERE. The EFC was applied on SPHERE a few years ago using the internal source (no turbulence). The contrast was improved by a factor of ~ 10 inside the control radius. However, because the technique required at this time the measurement of an empirical interaction matrix it was deemed time-consuming for being implemented in SPHERE. Associating EFC and PW as described above overcomes that limitation because no empirical matrix is needed. The purpose of a phase A would be to study the optimal combination of these techniques and propose a realistic implementation in SPHERE.

4.3 Coronagraphy

Coronagraphy was designed from the very beginning in SPHERE with an important constraint: reaching the highest contrasts at the shortest angular separations across a very large bandwidth. Instead of

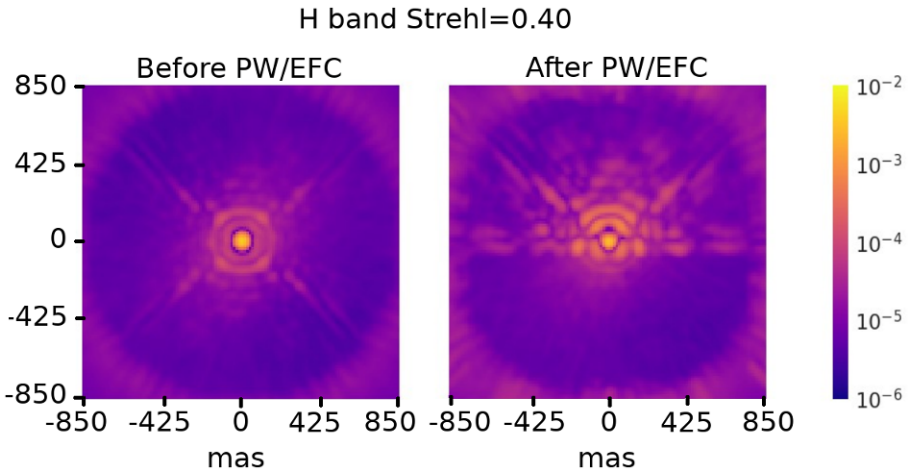

Figure 15: Numerical simulations of a long-exposure science coronagraphic image recorded in H-band with SPHERE assuming atmospheric turbulence and no quasi-static wavefront aberrations. Strehl ratio is 0.4. Left: before PW/EFC correction showing the stellar diffraction pattern limitation above the AO halo. Right: after minimization of the stellar intensity in the bottom of the DM influence area (called half dark hole).

focusing on a single design we implemented a suite of coronagraphic systems for various science goals, and in particular two designs were developed for SHINE, the Half Wave plate Four Quadrant Phase Mask (HW-4QPM, Rouan et al. 2000; Mawet et al. 2006) and the Apodized Lyot Coronagraph (Soummer 2005; Carbillet et al. 2011). Both were found to meet the requirements (central attenuation $>$100, contrast 10^{-4} at 3-5λ/D) in the lab tests but our strategy of having several concepts was proven efficient because the on-sky behaviour turned out to be different in the end. In particular the HW-4QPM was not able to reach the contrasts measured in the lab owing to various limitations (Beuzit et al. 2019, non common path aberration being the most likely culprit). For this reason SHINE is using the APLC. In that particular case, the twice smaller inner working angle of the HW-4QPM turned out to be a strong limitation.

While final contrasts result from a combination of optical starlight removal (the AO + coronagraph) and postprocessing (differential imaging), the action of the coronagraph is fundamental in that it sets the level of the photon noise in the image no matter the technique used to subtract the starlight afterwards. Therefore, for achieving the highest contrasts it is desirable to improve coronagraph performance, especially at the shortest angular separations where photon noise does matter (0.1-0.5"). However, a coronagraph, even if perfect, has an effect on the coherent part of the wavefront. Phase defects are escaping the action of the coronagraph and leak through the Lyot stop, hence setting the floor of speckles. Therefore, any improvement of a coronagraph should come with a higher correction of the phase (and possibly amplitude) aberrations by the xAO system. We have also identified that some coronagraphic designs can be very sensitive to the presence of dead actuators on the DM even if this effect can be mitigated (but not cancelled) with an adapted Lyot stop, as we did in SPHERE before shipping to Paranal in 2013.

In the SPHERE+ context we have started to explore several new designs, which are briefly described in Appendix A. These are alternative amplitude or phase apodized coronagraphs (new APLC, PAPLC, vAPP), pure focal plane phase masks (Vortex2, Vortex4) or apodized phase mask (RA Vortex2). Technology using liquid-crystal polymers now allows to manufacture broadband (JHK) phase coronagraphs (Doelman et al. in prep.). We investigated contrast performances, throughput, and sensitivity to aberrations.

To this end we performed simulations with identical assumptions as we did for the SPHERE FDR (Boccaletti et al. 2008), regarding phase defects residuals from the xAO, jitter (3mas rms), non common path (22nm rms), and dead actuators. These are preliminary simulations since the

whole parameter space in conditions relevant to SPHERE+ is still to be investigated, and should be phased with xAO simulations. AO correction is simulated with decorrelated phase screens hence does not account for temporal errors. We considered four specific cases with either SAXO1 (current correction) or SAXO2 (higher correction close to the axis), a very good seeing ($0.4''$) or a median value ($0.85''$). The performance are reported in terms of contrast profile (Fig.16) measured in a narrow H band ($\lambda = 1.6\mu$m, $\Delta\lambda$ =32nm), and corrected for throughput (which depends on coronagraph), and focusing on the region of interest ($< 0.4''$) where we aim for higher contrasts. The contrast of the various coronagraphs are very much dispersed on more than 1 order of magnitude in some cases. The worst cases are coronagraphs using pure focal plane phase masks (including the FQPM) due to their sensitivity to pointing errors and low frequencies aberrations, no matter which conditions are considered. On the contrary the most effective and robust are those based on pupil mask, with the PAPLC providing the best contrasts at the closest separations. Still, the current APLCs behave quite nicely except for the bump observed at $0.15''$ which can be compensated with the new APLC to lower down this diffraction peak, or by tweaking the phase on the DM. Even with the current system (SAXO1), there is a significant gain from going to $0.85''$ to $0.4''$ advocating the importance of the best seeing (and largest τ_0). Also, the performances of SAXO1 in excellent seeing is almost similar to SAXO2 in median seeing. Obviously, SAXO2 will be able to deliver higher contrasts much more frequently.

Overall the best coronagraph candidate for SPHERE+ amongst the considered possibilities is the PAPLC (Por et al., in prep.), which allows incursion at very short separations. Still, this coronagraph design is meant to be used with the IFS, hence with a limited field of view. More classical solutions like the current or the new APLC thus appear necessary. Interestingly, In the context of a phase A, we propose to investigate in more details the most relevant designs for each of the observing mode and to prepare a manufacturing/implementation plan.

4.4 Accessing higher spectral resolution

Deeper characterization of exoplanet atmosphere's to measure their constituents and ultimately to place constraints on their formation history would require significantly higher spectral resolution that what is currently offered by the IFS ($R_\lambda = 30 - 50$). SPHERE also implements a long slit spectrograph ($R_\lambda = 350$) but with limited contrast performance. Still, the large spectral coverage of the IFS achievable in a single snapshot has demonstrated high stability and high contrast performance. Taking advantage of both high spectral resolution and high contrast imaging has always been regarded as a crucial element for direct imaging of exoplanets (Sparks & Ford 2002), but a new approach has been recently proposed (Snellen et al. 2015) to boost simultaneously the level of characterization as well as the level of detection. Hence, it came as an evidence that SPHERE+ must allow higher spectral resolution. Two solutions are considered here, each covering a specific parameter space in terms of detection and characterization as presented in sections 4.4.1 and 4.4.2.

mentionner Hirise as a separate project

4.4.1 Medium-spectral resolution in the near-infrared

A medium resolution ($R_\lambda = 10^3 - 10^4$) integral field spectrograph in the near-infrared presents several advantages over the SPHERE IFS as recently demonstrated by the redetection of the planet β Pictoris b with VLT/SINFONI (Hoeijmakers et al. 2018). This technique involves the cross correlation with pre-defined templates or models of planet atmosphere's to disentangle the stellar from the planetary signals. Molecular species like H_2O, CH_4, CO, NH_3 have broad signatures in the near IR and can be already identified with low spectral resolution. But, the increase in spectral resolution from typically 50 to 5000 allows to exploit the finer spectral lines of these species hence providing a much cleaner rejection of the starlight by taking advantage of cross-correlation methods. The so-called "molecular-mapping" technique can significantly push the performance of SPHERE+ towards fainter exoplanets

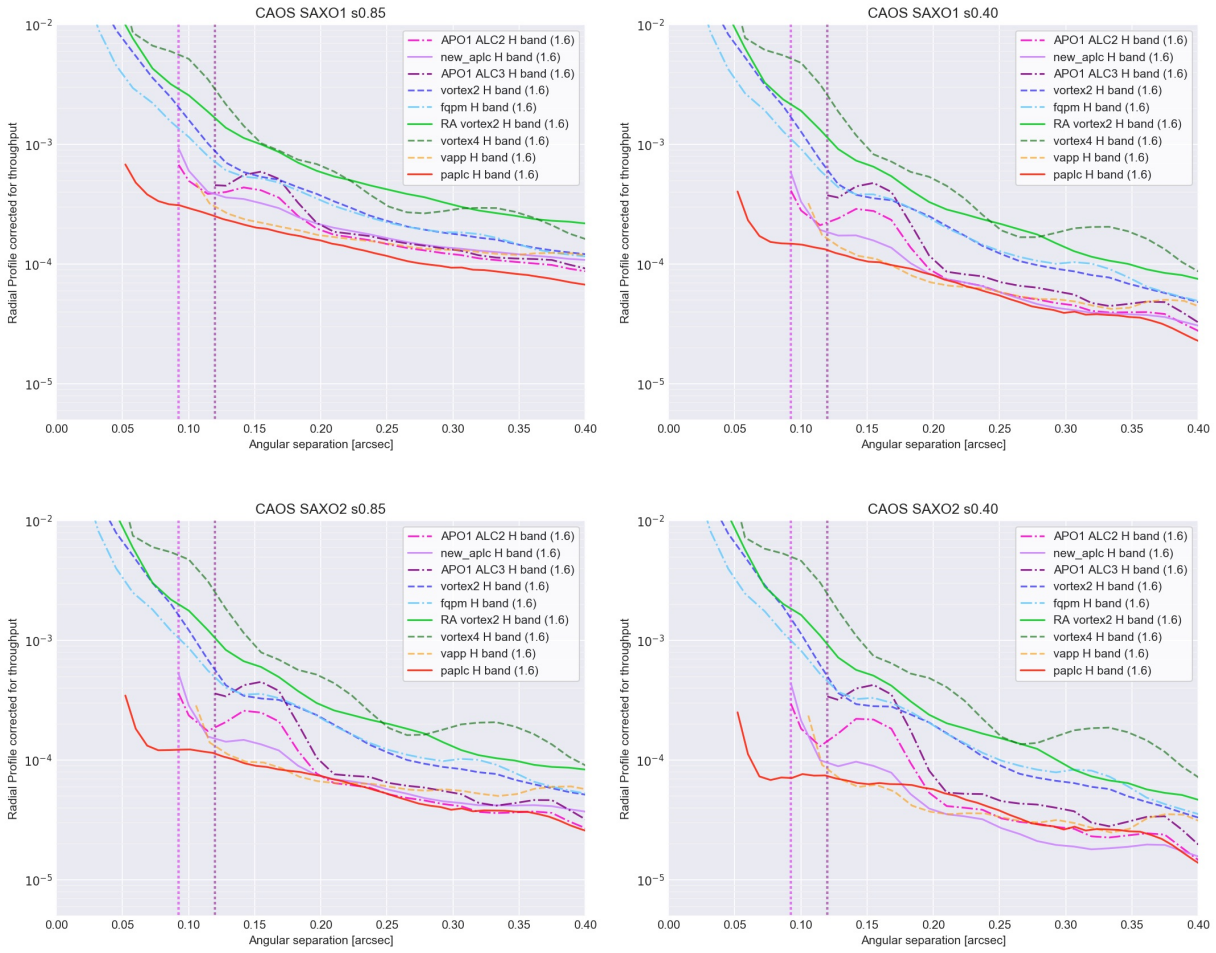

Figure 16: Mean contrast in the focal plane as a function of the angular separation for several type of coronagraphs in 2 seeing conditions 0.85″ (left) and 0.4″ (right) for the current AO system SAXO1 (top) and then for an upgraded systel SAXO2 (bottom).

and allows a higher degree of characterization (constraints on the C/O ratio for instance). Upgrading SPHERE with a such a facility should be regarded as equally important as pushing the xAO system to faster correction. It comes at a cost of a smaller field of view compared to IRDIS and IFS but still in line with the main science objectives of SPHERE+, which are dealing with the detection of exoplanets in the central arcsecond.

This mid-resolution IFS could be implemented as a deported fiber-fed spectrograph using an array of single-mode fibers combined with a dedicated apodizer optimized to maximize the coupling efficiency of the companions PSF into the fibers (Por & Haffert 2018; Haffert et al. 2018). The array of fiber could be optimized to sample a limited region of the focal-plane, e.g. 10x10 λ/D or 20$\times$20 λ/D. The infrared beam could be picked-up at the same location as is foreseen for the project HiRISE (see Sect. 4.4.2). The HiRISE study already foresees the possibility to have another system on the backplate of the HiRISE vertical board. Preliminary simulations show that a sensitivity gain of several magnitudes could be obtained very close to the star with such a system (Fig. 17), but a more detailed study is required to identify the limitations of such a system. Another key aspect would be the feasibility of an array of fibers optimized for the K-band if this spectral window reveals to be more interesting from the astrophysical point of view. For the H-band, standard silica fiber bundles are already manufacturable.

Phase A will allow a trade-off of relevant parameters like FoV, spectral resolution, size and mass, for a mid-resolution IFS.

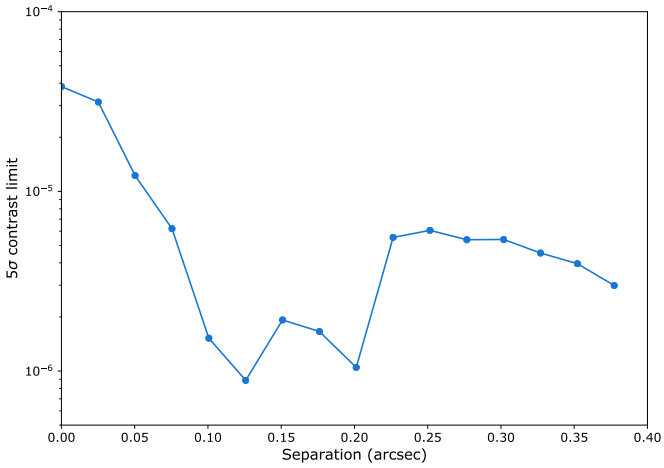

Figure 17: Simulated performance (calculated in 5 σ contrast) for a mid resolution spectrograph (Y band R=10000), assuming a planet of 1200K, log(g)=2.5, at various separations, and a 6000K, 11th magnitude central star. The data are processed similarly as in Hoeijmakers et al. (2018).

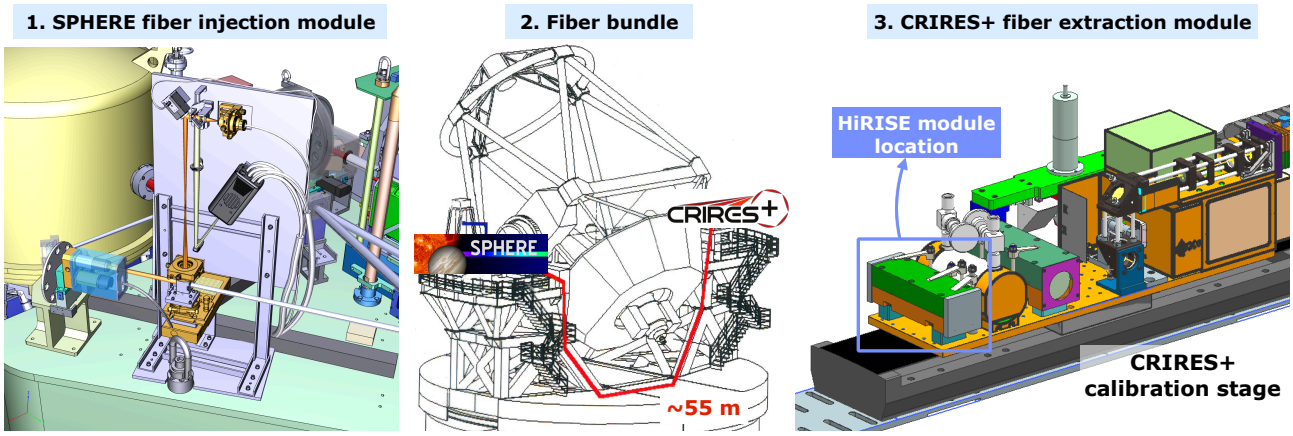

Figure 18: Proposed implementation for HiRISE. The coupling is composed of three major parts: (1) a fiber injection module implemented in SPHERE to pick-up the light of a known exoplanet, (2) a fiber bundle that transmits this light from SPHERE to CRIRES+, and (3) a fiber extraction module in CRIRES+ that brings the light in the calibration stage located at the entrance of the instrument

4.4.2 High-spectral resolution in the near-infrared

Very high-spectral resolution ($R_\lambda = 10^5$) in the near-infrared would provide significantly improved characterization capabilities for known giant exoplanets, like the determination of their orbital and rotational velocities and much more detailed spectral characterization. Providing such resolutions in the form of an IFS would require a complicated and costly spectrograph, so it has been suggested that for characterization purposes the signal of a known planet could be picked-up in SPHERE and fiber-fed to a spectrograph, either existing or dedicated. The VLT-UT3 will soon host the refurbished and improved high-resolution near-infrared spectrograph CRIRES+, which provides a unique opportunity to implement a high-resolution mode for direct exoplanet characterization on the UT3. This possibility is being proposed as a dedicated project called HiRISE[4] and already funded through an ERC starting grant (PI Vigan, grant agreement #757561). HiRISE proposes to implement a fiber injection module in the near-infrared arm of SPHERE, a ZBLAN fiber bundle going from Nasmyth A to Nasmyth B,

[4] http://astro.vigan.fr/hirise.html

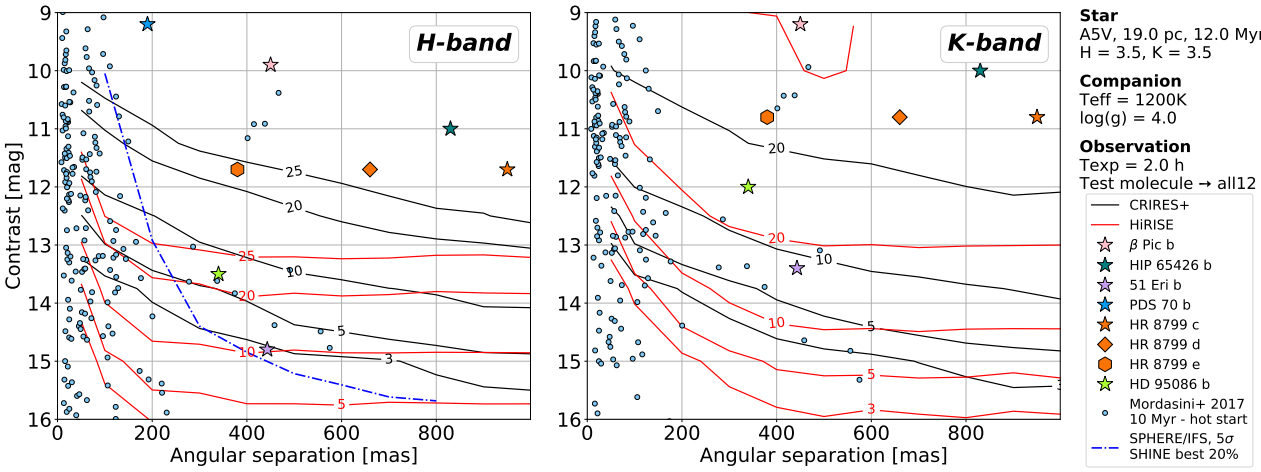

Figure 19: Expected SNR of the CCF for 2 hours of integration time with CRIRES+ (black lines) and HiRISE (red lines) in H-band (left) and K-band (right) as a function of contrast and angular separation around a β Pictoris-like star (H=3.5, 19 pc, 12 Myr) and for a HIP 65426 b-like companion (1200K, log(g)=4.0). Well-known directly-imaged companions are overplotted, as well as results from state-of-the-art population synthesis models (Mordasini et al. 2017) and the average of the 20% best SPHERE/IFS 5σ detection limits from the SHINE survey (Chauvin et al. 2017). The SNR is computed by cross-correlation of a full ATMO model including 12 different atmospheric species (Tremblin et al. 2015) to the noisy data CRIRES+ or HiRISE data generated by the end-to-end simulation (Otten et al. in prep.).

and a fiber extraction module in the calibration stage of CRIRES+ (Figure 18; Vigan et al. 2018). There are no show-stoppers in the feasibility of the project and the implementation could be foreseen on a much shorter timescale than a more general SPHERE upgrade. The project is currently at the end of its phase A and is foreseen to be implemented as a demonstrator. Using a dedicated diffraction-limited, fiber-fed spectrograph is also explored in parallel (Bourdarot et al. 2018). This approach would be compatible with HiRISE: instead of going to CRIRES+, the science fibers coming from the injection module would go to a small spectrograph sitting on the Nasmyth platform as SPHERE. The main benefit would be a gain in throughput, which is the driving parameter in the performance of HiRISE. In addition to characterization of known companions, simulations have showed that HiRISE should enable the detection of yet unknown planets at much shorter angular separation, provided that the position is known beforehand (e.g. from ESA/*Gaia*). The gain in sensitivity is estimated to be up to 6 magnitudes better than SPHERE at separations < 200 mas (Fig. 19).

While the HiRISE project is independent, we fully endorse such an evolution towards better characterization of exoplanet's atmosphere and SPHERE+ should be designed such as to faciliate or improves the HiRISE concept.

4.4.3 High-spectral resolution in the visible

The dedicated study of Lovis et al. (2017) has proposed to combine SPHERE and ESPRESSO in the visible to enable the detection of planets in reflected light, and in particular proxima Cen b. Again this proposition relies on the high-angular resolution and high-contrast provided by SPHERE, combined with the extremely high-spectral resolution of ESPRESSO. However, this would require a significantly upgraded AO system in the visible, an appropriate coronagraph and a massive amount of observing time over several years. In this proposition, the main show-stopper remains the AO system, which would need to run 3 to 5 times faster to reach the Strehl necessary to enable sufficient stellar attenuation with a coronagraph at 2 λ/D in the visible. This is why this option is not currently considered as fitting in the timeframe of SPHERE+.

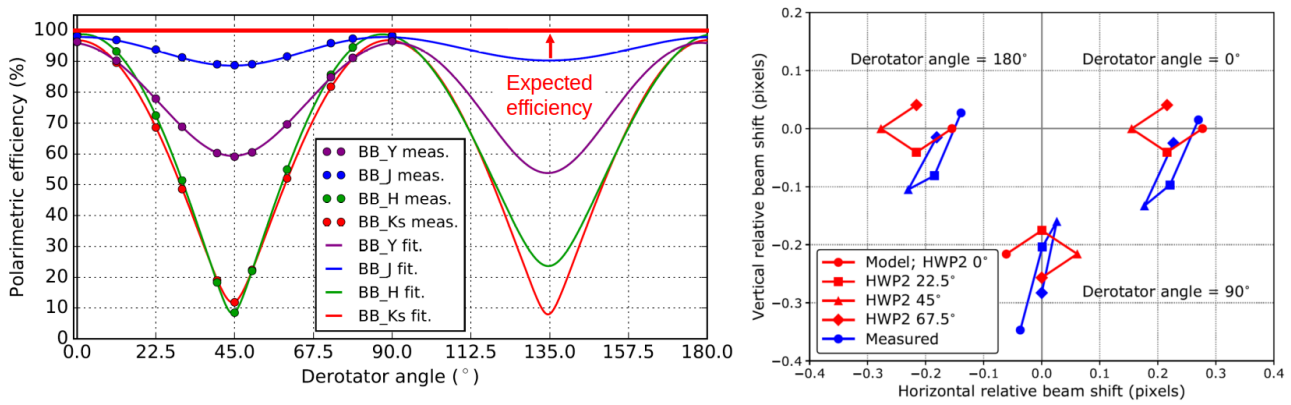

Figure 20: *Left:* Polarimetric efficiency of IRDIS depending on the derotator angle for multiple broad-band filters (van Holstein et al., subm.). *Right:* ZIMPOL beam-shift offsets between the two orthogonal polarization directions depending on derotator position (van Holstein et al., in prep.).

4.5 Polarimetry

As previously discussed, a large part of the SPHERE science return is provided by the study of circumstellar disks in various stages of their evolution. The workhorse technique for these studies is polarimetric differential imaging with the IRDIS and ZIMPOL sub-systems in the near-infrared and visible light respectively. While this technique already produces spectacular results, we propose two improvements that can greatly boost the performance and expected science output of this observing mode.

4.5.1 Influence of the derotator on polarimetric performance

An issue concerning all polarimetric sub-systems is the current implementation of the instrument derotator. The coating of the derotator mirrors was selected to guarantee high reflectivity and thus high throughput of the system. However, the coating was not optimized to minimize retardance. This has a dramatic effect on the IRDIS polarimetric efficiency (i.e. the ratio of measured polarization degree / the incident or true polarization degree). Depending on the position of the derotator and the selected bands, polarimetric efficiency drops down to 10% (see Fig. 20). In field tracking mode this means the derotator angles have to be adjusted according to the position of the target on sky. Especially for targets that are observed at low airmass ($<$1.2), frequent manual adjustments are needed making field tracking observations at high altitudes cumbersome for ESO personel, and prone to errors in the execution. Wrong derotator angles in service mode observations have already led to a significant loss of observation time. This is particularly problematic, as most disk observations now focus on faint T Tauri stars, which have to be observed at good weather conditions and thus are executed in service mode. Even when care is taken, it is often not feasible to avoid a loss of up to 20% of polarimetric efficiency due to the frequent changes in derotator angle that are required. Even more interesting than doing polarimetric imaging in field-tracking mode is to do it combined with pupil tracking as has been illustrated by van Holstein et al. (2017). We then have the possibility to combine polarimetric differential imaging with angular differential imaging and therefore can do a combined search or characterization of circumstellar disks and planets simultaneously. In pupil tracking mode we cannot select a derotator offset because the pupil needs to be aligned with the Lyot stop. Therefore, for this potentially most productive imaging mode of SPHERE we have to rely on tight sidereal time constraints to obtain decent derotator angles and corresponding favorable polarimetric efficiencies. Such time constraints limit the applicability of this mode and make it much more complex for the observer to use. Combining the general efficiency loss with the human-error factor in setting the correct time-dependent derotator position leads to significantly increased integration times to achieve

the individual science goals or performance that is below expectation.

For the ZIMPOL sub-system the derotator introduces beam-shifts due the Goos–Hänchen effect (Schmid et al. 2018). These beam-shifts are on the order of 0.1 to 0.3 detector pixel (see Fig. 20). These are relative shifts between the different polarization directions. Due to these beam-shifts, polarimetric differential imaging post-processing is producing strong noise artifacts at the smallest angular separations (< 0.2"). These smallest separations are in fact the most interesting regions for the detection of (dust depleted cavities in) small circumstellar disks as well as reflected light from evolved extrasolar planets close to their host stars (i.e. the original science case of ZIMPOL).

We wish to address both of these adverse effects to two of the sub-systems by replacing the current derotator with one that is identical except for its coating properties. The decrease in polarimetric efficiency shown in Fig. 20 is predominantly due to the retardance of this coating. We are currently investigating the feasibility of improving this retardance for a broad wavelength range, while keeping all other specifications (e.g. reflectivity) at the same level.

As an alternative to replacing the derotator we are investigating the possibility to insert an additional half-wave plate, downstream of the derotator. This would allow for retardance of the derotator to be compensated. This may however require rather large half wave plate since we are dealing with a wide beam at this position.

4.5.2 Replacement of the IRDIS beamsplitter

Currently the beamsplitter used in IRDIS is roughly non-polarizing. For polarimetric measurements, two wire-grid polarizers are thus inserted in order to filter the light for orthogonal polarization directions from the predominantly unpolarized beam. This means that we currently use only half of the photons in polarimetric mode that we receive, which leads directly to a 50% increase in necessary integration time. This is particularly bothersome for the potentially most valuable observing mode combining pupil tracking and polarimetric differential imaging. This mode is ideal for surveys of particularly young systems to find protoplanets still embedded in their circumstellar birth-disks as was for example observed recently around the young star PDS 70 (Keppler et al. 2018). The combination of polarization and total intensity (angular) differential imaging allows here to discern planets from disk features.

For the SPHERE+ upgrade we thus investigate the possibility of replacing the current IRDIS beamsplitter with a polarizing beamsplitter. Polarizing beamsplitters have typically a polarimetric efficiency of 90 %, drastically increasing the throughput of the system in polarimetric mode. This will allow for polarimetry to be included as a standard characterization method in future large exoplanet surveys for free, while not adversely affecting standard imaging modes. Having such a device may also allows focal plane wavefront sensing in combination with phase-mask coronagraphs like the VVC.

ZIMPOL

4.6 Fast visible camera

A fast camera in the visible can allow to address a specific science case related to accreting planets as discussed in section 3.1. Since no major raw contrast improvement is expected in the visible due to the choice of a second stage xAO interlaced in the IR beam, we propose a fast-imaging visible channel for SPHERE, which relevance is to be studied in phase A. SLOTS (Sphere Looking Objects Through Speckles) is designed around a high frame rate (acquisition frequency up to 1 kHz) and very low readout noise detector, following the concept used for the SHARK-VIS instrument at LBT. The high cadence allows us to freeze the atmospheric turbulence evolution, whose timescales are of the order of a few ms at visible wavelengths (Stangalini et al. 2017). This enables to perform a post-facto correction of the residual jitter based on a Gaussian fit of the PSF core, which maximizes the spatial resolution and improve the peak contrast of the faint target (Fig. 21). Moreover, a number

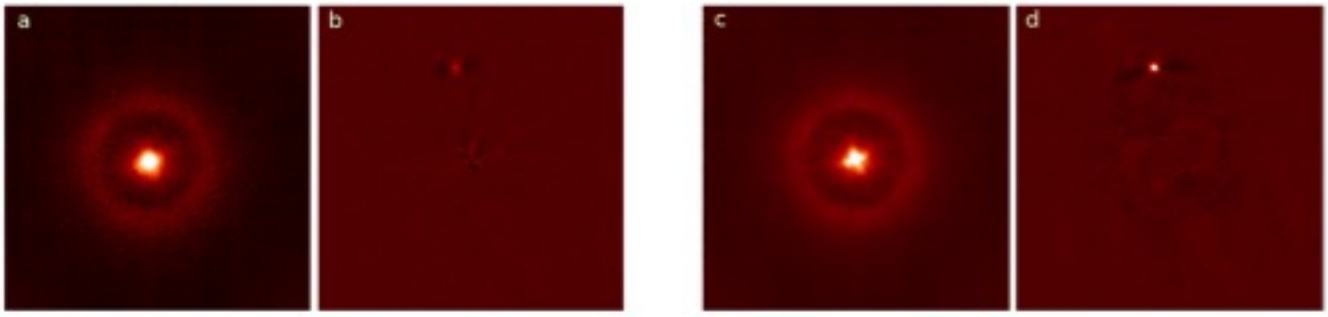

Figure 21: Comparison between classical long-exposure (left) and fast-imaging (right) results, based on observations of HD 8375 made at LBT with the SHARK-VIS Forerunner instrument at 6500Å. Left panels display the average image assuming 10s ZIMPOL-like long exposures (a) and the result of PCA post-processing (b), which evidences the companion with an intrinsic contrast of about $3.10^{-}3$ at a SNR of 25 (separation $\sim$200 mas). The right panels show the average (c) and iPCA image (d) using fast-imaging at 1kHz cadence: peak and sharpness of the companion are significantly improved, with an increased SNR of 100 (same linear color scale for panels b and d).

of post-processing techniques can be applied that fully exploit the spatio-temporal information contained in the frame sequences, such as SFADI (Speckle-Free Angular Differential Imaging, Li Causi et al. 2017, which explores the dark sky regions in between the speckles in the single frames), RQA (Recurrence Quantification Analysis, Stangalini et al. 2017), MFBD (Multi-Frame Blind Deconvolution), and iPCA (incremental Principal Component Analysis) on a very large set of frames. These techniques have already been successfully tested with the SHARK-VIS Forerunner data at LBT and showed significant improvements compared to results obtained with longer exposures and standard data processing methods, with contrasts as low as 2.10^{-5} measured on-sky at 100 mas from the central star (Pedichini et al. 2017) and angular resolutions down to 16 mas (resolved components of α And, Mattioli et al. 2019).

Feeding of SLOTS will be achieved by folding the current ZIMPOL foreoptics path and by using its coronagraph mask wheel. The folded focal plane (may be a coronagraph by using the current ZIMPOL occulter wheel or a direct imager) is focused on the EM-CCD detector of an OCAM2K unit provided by First Light or that of an ANDOR IXON. A movable folding mirror allows the light beam to use the original coronagraph of ZIMPOL and to feed the camera at 4 or 7.5 mas/pixel by means of two different deployable "refocusing lenses". Camera lenses will be derived from current ZIMPOL collimator doublet technology (CaF2+ S-NSL36). A further stop wheel can be added with the replica of the original pupil stops already present in the ZIMPOL pupil wheel in case coronagraphy with SLOTS is implemented.

4.7 Observing strategy, data reduction, and tools

High contrast imaging has benefit a lot from specific observing strategies. Starting from 2006-2008, the use of the pupil-stabilized mode has been decisive to provide data sets with very good stability on which dedicated algorithms could be applied and led to the discoveries of the first famous giant planets, HR 8799 bcde and β Pic b. For this reason, SPHERE was designed with a strong stability requirement to allow for very high contrasts. SPHERE+ will keep this requirement as a major constrain in the design. In that respect, stability on the timescale of an observing block is crucial to fully exploit ADI. However, as we target closer angular angular separations for exoplanet science, or since we aim to retrieve unbiased total intensity images of disks, ADI is not necessarily optimal and RDI might be more appropriate. In that case the important timescale for stability is much longer. The solution to reach this stability is not only a matter of instrument design but the operation is a key point to provide homogeneity in the data quality. Therefore, a large survey with SPHERE+ must take advantage of the

best conditions (lowest seeing/ largest coherence time) which is only possible in service.

Data reduction is intimately related to the observing strategy. The SPHERE consortium has developed several tools for making the best use out of the data (Specal, Andromeda, Galicher et al. 2018; Cantalloube et al. 2015), now integrated into the SPHERE Data center (Delorme et al. 2017a). The SPHERE Data center is organized around two main tools: the Processing Center (PC)[5] and the Target DataBase (TDB)[6]. The PC is oriented toward data processing and reduced data distribution organized around observations and instruments, while the TDB is oriented toward the distribution of advanced data products organized around targets and surveys. The TDB represents also the main SPHERE Data Center link to the Virtual Observatory. The SPHERE+ project will completely rely on this advanced reference center for high-contrast imaging, which is now extending its development in the context of machine learning (Gomez Gonzalez et al. 2018). Finally, optimal interpretation of the data for exoplanets requires atmosphere and/or evolutionary models to compare with the data. Our teams have developed a specific tool (ExoREM, Charnay et al. 2018), which is expected to evolve to match the new functionalities of SPHERE+ (higher spectral resolution in particular).

5 Need for a Phase A

The young field of exoplanetary science has drastically expanded in the past years. Twenty five years ago, the only planets we knew were the ones of our Solar System. Today, thousands of exoplanets have been discovered since the 51 Peg discovery (Mayor & Queloz 1995) and, with the diversity of systems found (Hot Jupiters, irradiated and evaporating planets, planetary orbits misaligned with stellar spin, planets in binaries, telluric planets in habitable zone, discovery of Mars-size planets...), the theories of planetary formation and evolution have drastically evolved to digest these observing constraints. Although the detection bio-signatures in the atmosphere of a nearby Super Earth is becoming a strong motivation for future projects, we are still missing the full vision and some key fundamental questions lack answers. With this perspective, the SPHERE+ top science goals are to investigate: i/ the existence of one or several mechanisms to form giant planets pushing today's SPHERE horizon, ii/ the physics of accretion to form their gaseous atmospheres and the connection with circumstellar disk properties and structures, iii/ the physical properties of young Jupiters and their time evolution, and iv/ the impact of dynamical evolution in crafting planetary system architectures to create favorable conditions for the formation of telluric planets capable of hosting life. These science cases are unique in the thematic of exoplanets and disks, and can be reached by building on our rich expertise in designing, integrating, testing and exploiting SPHERE to reach new astrophysical depths with the SPHERE+ upgrade.

The connected requirements to reach the SPHERE+ science goals can be summarized as reaching closer and deeper contrasts, accessing fainter targets and extending the current SPHERE detection/characterization capabilities to higher spectral resolution. To reach them, we have conceived a coherent instrumental project including an upgrade of the SAXO system with a double-stage xAO, the optimized calibration and compensation of the non-common path aberrations, the implementation of new generation of coronagraphs, finally the coupling to medium and high-resolution spectrograph in the near-infrared, and a fast-camera in visible. The exact list of sub-systems which SPHERE+ will include is to be studied in phase A, and depends on several parameters (scientific relevance, mass allocation, cost, time of development...). SPHERE+ builds on the existing expertise of the European community including the former SPHERE consortium, plus new partners (Appendix B), with demonstrated capacity in this field of research, both on astrophysical and technical aspects. SPHERE+ is proposing a gradual and coherent upgrade to SPHERE with mitigated risks, yet a strong scientific impact. Most of the modifications we intend to bring are essentially transparent so that the system can still operate in its default configuration, especially at the level of the AO system but also regarding

[5]http://datacenter.osug.fr

[6]https://www.lam.fr/cesam

the availability of the main instruments IRDIS and IFS (which will benefit from AO upgrade too). All additional items can be assembled, tested and validated in Europe before being shipped to Paranal. On-sky validation will obviously requires technical time at the telescope but we anticipate a very short downtime of SPHERE, which still can be offered most of the time. The development of SPHERE+ can be organized as incremental steps from the most straightforward to the most complex, each with independent timeline and minimal impact on the current system, with the ability to step back to the original configuration.

- The first step consists of upgrading some existing elements with minimal development time and moderated costs: coronagraphs, algorithms for the correction of NCPA, and polarimetric components. The implementation of this phase will be fast as the underlying concepts are at a high technological readiness level.

- The second step focuses on the implementation of new instruments, essentially the spectroscopic capabilities with a new medium resolution spectrograph and a coupling to CRIRES+ to achieve higher spectral resolution, and a fast visible camera.

- The final step represents a major upgrade with the addition of a second xAO stage, and is certainly the most demanding in terms of resources and costs. It relies on the existing components, namely SAXO, still operating with the current HODM.

The full performance of SPHERE+ will be effective when all steps will be completed. However, each step can be validated independently, and each will enable noticeable and gradual improvement of performance. In terms of cost and time estimate, a Phase A is needed to work out the numbers, but a very first order evaluation (Tab. 1) indicates a total of 3.3 Million euros project (half of it being allocated to SAXO2), and 4 years of development to complete the 3rd phase. The decision to replace the HODM being independent from the SPHERE+ project, its cost is not accounted in the SPHERE+ total cost and remains optional.

In a context of intensive development, strong competition, and limited resources, SPHERE+ brings a significant evolution of SPHERE in synergy with other facilities from the ground and in space in the exoplanetary research field (ALMA, GRAVITY, CRIRES+, ESPRESSO, ERIS, MUSE, *Gaia*, *JWST*). SPHERE+ is designed to minimize the impact on current operation, and to maintain a world-leading position of the VLT for the upcoming decade. SPHERE+ will prepare the advent of the ELT science and instrumentation in 2026 by offering an extremely competitive survey planet imager for future in-depth characterization with the ELT of the most promising and challenging planetary systems. It will offer the opportunity to explore and consolidate new developments to address the most ambitious goals of a second generation instrument like the PCS concept to discover and characterize Super Earths with the ELT.

The scientists and institutes involved in this proposal have shown unique expertise worldwide in designing, developing, testing and exploiting high contrast instruments on-sky. One of the successes of SPHERE, in terms of scientific productivity, as opposed to its competitors, is definitely the versatility, the number of modes offered to a large community and the unprecedented stability in operation. With SPHERE+, we certainly intend to reproduce the same approach. **In that perspective, a Phase A will offer the adequate framework to structure the new SPHERE+ consortium to carry out the relevant trade-off studies, the cost and resources estimation, and to establish a management plan for a future Phase B.**

Table 1: Implementation and preliminary cost estimates for SPHERE+

Phase	Component	Cost (M€)	Description
1	Coronagraphy/NCPA	0.1	new APLC, PAPLC, ZELDA
1	Polarimetry	0.3	derotator, beam splitter
2	mid-R spectrograph	1.0	detector, HW
2	HiRISE	0.2	SPHERE/CRIRES+ modules, fiber
2	fast camera	0.2	detector, HW
3	SAXO2	1.5	DM, Pyr-WFS, detector, RTC
SPHERE+ Total		3.3	
HODM1 replacement (optional)		1.5	new HODM, electronics

A SPHERE+ IR coronagraph performance simulations

A.1 Coronagraph description

A comparative study including nine coronagraphs has been carried out to identify solutions with the highest gain in performance. Three of these configurations are currently available in SPHERE: APO1-ALC2 in IRDIFS mode (YJ+H2H3), and APO1-ALC3 in in IRDIFS-ext mode (YJH+K1K2), are the two APLC configurations that are used most of the time for SHINE, and the four-quadrant-phase mask (FQPM) is available but not offered due to on-sky performance lower than expected. The other six considered coronagraphs are described below and their main features are listed in Tab. 2:

- a new APLC design (N'Diaye & Carlotti) consisting of a binary amplitude apodization mask combined with the ALC2 focal plane occulting mask (185 mas diameter). The apodization is optimized for imaging at H band with 20% bandwidth. The inner working angle (IWA) is the same as the APO1-ALC2 in H band, i.e. 2.5 λ/D. Outer working angle (OWA) is 20 λ/D, that is 0.9″ in the H band. Manufacturing of the pupil apodizer based on microphotolithography is a well known process.

- a vector vortex of charge 2 (Vortex2), simulated by a vortex phase mask (no leakage term taken into account as the leakage due to the central obstruction is dominant). Liquid crystal polymers are the most appropriate manufacturing option, as it can produce broadband components (J to K). A more complex version including a double grating (dgVVC, Doelman D., Snik F.) to split the polarizations could reduce the intrinsic leakage term and would make focal plane wavefront sensing possible, based on the analysis of the two polarization images.

- a vector vortex of charge 4 (Vortex4), simulated by a vortex phase mask. Same manufacturing considerations as for the vector vortex of charge 2.

- a ring apodized vortex coronagraph (RAVortex2, Mawet et al. 2010) consisting of an amplitude apodization with gray transmission in an annulus, combined with a corresponding over-sized Lyot stop, and a vortex phase mask of charge 2 in the focal plane. The entrance pupil apodization allows to remove the diffraction due to the central obstruction, at the cost of a reduced transmission efficiency.

- a vector apodized phase plate coronagraph (vAPP, Bos et al. 2018; Otten et al. 2017), consisting in a pupil plane phase apodization. The phase plate includes a grating to split the polarizations, inducing two off-axis coronagraphic images. This coronagraph works as a PSF reshaper, digging a dark hole on one side of each stellar PSF. Neutral density could be added in the focal plane in order to dim the stellar light or the central peak can be used for wavefront sensing.

- a phase-apodized pupil Lyot coronagraph (PAPLC, Por 2017), consisting in a phase apodization including a grating, an amplitude focal plane mask occulting half of the FoV of the two PSFs, and a Lyot stop. As in the vAPP case, this coronagraph is more appropriate for IFS mode, since the stellar images are offset.

The last two coronagraphs include a phase apodization with a grating that splits the two polarizations in two locations in the field of view, at separation that scales with λ/D. To avoid blurring, this kind of coronagraph is thus more appropriate for operation in narrow spectral bands, that is in the IFS mode. On each stellar PSF, half of the field of view (FoV) is accessible for exoplanet / disk detection. In this study, only one polarization has been simulated, which means that flux contamination by the other image is not taken into account.

A.2 Simulation assumptions

In order to consistently compare the performance of all coronagraphs, they were simulated in the same aberration conditions and in the same wavelength band (at $\lambda = 1.6\mu$m, $\Delta\lambda = 32$nm), even though some of them are also meant to be used in broad band imaging mode (APLC, VVC). Results were shown in Fig. 16 where planet throughput are accounted for (Fig. 22). Residual aberrations include:

- aberrations due to the telescope mirrors (perfectly filtered by the AO system),
- six dead actuators (modeled by phase errors with a Gaussian profile). This model might be slightly pessimistic, and simulations were also carried out without this contribution, showing the benefit of a fully working deformable mirror.
- non common path aberrations (NCPA), including 3 mas rms jitter, and a residual phase map as measured by ZELDA after NCPA correction (22nm rms in total).
- turbulence residuals after SAXO correction. To simulate turbulence residuals, 100 coronagraphic images were averaged, each with an independent turbulent phase screen drawn from post-AO Power Spectral Density generated by the SPHERE simulator CAOS. SAXO1 corresponds to the current AO system configuration (Shack Hartman 40x40 WFS, 1.2kHz) while SAXO2 includes a second correction stage (pyramid 24x24 WFS, 2.5kHz) providing a better correction close to the star.

Coro.	IWA λ/D	OWA λ/D	Max planet throughput %	comments
New APLC	2.5	20	38	Manufacturing: Microphotolithography ($<$ 10k euros)
Vortex2	1.4	-	44	Manufacturing: liquid crystal polymers Double grating version $\sim$30k euros compatible with focal plane WFS
Vortex4	3.0	-	42	-
RAVortex2	1.5	-	26	Double grating version $\sim$40k euros
vAPP	2.5	17	24	Two coro. images off-axis with half FoV (centered on $\pm$[12.9, 8.3] λ/D) Compatible with focal plane WFS
PAPLC	1.6	15	30	Two coro. images off-axis with half FoV (centered on $\pm$[25.4,-1.2] λ/D) Compatible with focal plane WFS

Table 2: Coronagraph features

B Supporting institutes

The SPHERE+ project is supported by the institutes of the SPHERE consortium augmented with new partners as follows :

- CRAL, Univ. Lyon; IPAG, Univ Grenoble-Alpes; Lagrange, Obs. Côte d'Azur; LAM, Univ. Aix-Marseille; LESIA, Obs. Paris; ONERA, in France
- MPIA in Germany
- NOVA, Univ. Leiden; and NOVA, Univ. Amsterdam, in The Netherland
- INAF, Obs. Padova; INAF, Obs Roma; INAF, Obs. Brera, in Italy
- Obs. Geneve, and ETH Zurich in Switzerland
- STAR, Univ. Liège, in Belgium

Other partners could be seek in phase A.

These institutes have broad interests in the context of exoplanets, disks and science topics, which can take advantage of high contrast imaging. They have technical expertise covering all the aspects of the SPHERE+ project as follows :

- system analysis
- extreme AO, deformable mirror technology, Real Time Computer
- wavefront sensing with pyramid
- wavefront correction in pupil and focal plane
- coronagraphs, integral field spectrographs
- high precision polarimetry and associated components

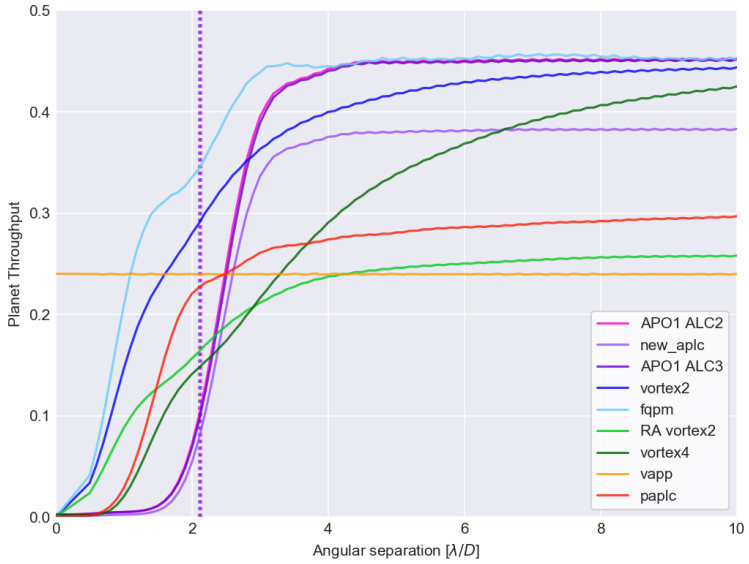

Figure 22: The planet throughput is computed by integrating the flux in a disk of diameter 1.4 λ/D, normalized by the flux of the PSF.

- Instrument Control Software
- high-cadence visible detectors
- optics, cryogenics
- post-processing, data handling, and modeling

References

Alcalá, Manara, Natta, et al. 2017, A&A, 600, A20
Andrews, Huang, Pérez, et al. 2018, ApJ, 869, L41
Antoniucci, Podio, Nisini, et al. 2016, A&A, 593, L13
Bae, Pinilla, & Birnstiel. 2018, ApJ, 864, L26
Baudoz, Dorn, Lizon, et al. 2010, in Proc. SPIE, Vol. 7735, Ground-based and Airborne Instrumentation for Astronomy IV, 77355B
Benisty, Juhasz, Boccaletti, et al. 2015, A&A, 578, L6
Benisty, Stolker, Pohl, et al. 2017, A&A, 597, A42
Beuzit, Vigan, Mouillet, et al. 2019, arXiv.org 1902.04080v1
Boccaletti, Carbillet, Fusco, et al. 2008, in Proc. SPIE, Vol. 7015, Adaptive Optics Systems, 70156E
Boccaletti, Sezestre, Lagrange, et al. 2018, A&A, 614, A52
Boccaletti, Thalmann, Lagrange, et al. 2015, Nature, 526, 230
Bonnefoy, Milli, Ménard, et al. 2017, A&A, 597, L7
Bonnefoy, Perraut, Lagrange, et al. 2018, A&A, 618, A63
Bonnefoy, Zurlo, Baudino, et al. 2016, A&A, 587, A58
Bordé & Traub. 2006, ApJ, 638, 488
Bos, Doelman, de Boer, et al. 2018, in Proc. SPIE, Vol. 10706, Advances in Optical and Mechanical Technologies for Telescopes and Instrumentation III, 107065M
Bottom, Wallace, Bartos, Shelton, & Serabyn. 2017, MNRAS, 464, 2937
Bourdarot, Le Coarer, Mouillet, et al. 2018, in Proc. SPIE, Vol. 10702, Ground-based and Airborne Instrumentation for Astronomy VII, 107025Y
Bryan, Benneke, Knutson, Batygin, & Bowler. 2018, Nature Astronomy, 2, 138
Cantalloube, Mouillet, Mugnier, et al. 2015, A&A, 582, A89
Cantalloube, Por, Dohlen, et al. 2018, A&A, 620, L10
Carbillet, Bendjoya, Abe, et al. 2011, Experimental Astronomy, 30, 39
Carry, Vachier, Berthier, et al. 2019, A&A, 623, A132
Charbonneau, Brown, Noyes, & Gilliland. 2002, ApJ, 568, 377
Charnay, Bézard, Baudino, et al. 2018, ApJ, 854, 172
Chauvin, Desidera, Lagrange, et al. 2017, A&A, 605, L9
Chauvin, Gratton, Bonnefoy, et al. 2018, A&A, 617, A76
Chauvin, Lagrange, Dumas, et al. 2004, A&A, 425, L29
Cheetham, Bonnefoy, Desidera, et al. 2018a, A&A, 615, A160
Cheetham, Ségransan, Peretti, et al. 2018b, A&A, 614, A16
Cheetham, Samland, Brems, et al. 2019, A&A, 622, A80
Christiaens, Casassus, Absil, et al. 2019, MNRAS, 486, 5819
Close, Follette, Males, et al. 2014, ApJ, 781, L30
Crossfield, Biller, Schlieder, et al. 2014, Nature, 505, 654
Davies, Esposito, Schmid, et al. 2018, in Proc. SPIE, Vol. 10702, Ground-based and Airborne Instrumentation for Astronomy VII, 1070209
de Boer, Salter, Benisty, et al. 2016, A&A, 595, A114
Delorme, Meunier, Albert, et al. 2017a, in SF2A-2017: Proceedings of the Annual meeting of the French Society of Astronomy and Astrophysics, Di
Delorme, Schmidt, Bonnefoy, et al. 2017b, A&A, 608, A79
Demory, Gillon, Seager, et al. 2012, ApJ, 751, L28
Dong, Zhu, Rafikov, & Stone. 2015a, ApJ, 809, L5
Dong, Zhu, & Whitney. 2015b, ApJ, 809, 93
D'Orazi, Gratton, Desidera, et al. 2019, Nature Astronomy, 3, 167
Feldt, Olofsson, Boccaletti, et al. 2017, A&A, 601, A7

Fétick, Jorda, Vernazza, et al. 2019, A&A, 623, A6
Flock, Nelson, Turner, et al. 2017, ApJ, 850, 131
Fusco, Rousset, Sauvage, et al. 2006, Optics Express, 14, 7515
Galicher, Baudoz, Rousset, Totems, & Mas. 2010, A&A, 509, A31
Galicher, Boccaletti, Mesa, et al. 2018, A&A, 615, A92
Ginski, Stolker, Pinilla, et al. 2016, A&A, 595, A112
Give'On, Belikov, Shaklan, & Kasdin. 2007, Optics Express, 15, 12338
Gomez Gonzalez, Absil, & Van Droogenbroeck. 2018, A&A, 613, A71
Gratadour, Rouan, Grosset, Boccaletti, & Clénet. 2015, A&A, 581, L8
Gratton, Ligi, Sissa, et al. 2019a, A&A, 623, A140
Gratton, Ligi, Sissa, et al. 2019b, A&A, 623, A140
Haffert, Bohn, De Boer, et al. 2019, arXiv.org, 211
Haffert, Por, Keller, et al. 2018, arXiv e-prints, 1803.10693
Hanuš, Marchis, Viikinkoski, Yang, & Kaasalainen. 2017, A&A, 599, A36
Hoeijmakers, Schwarz, Snellen, et al. 2018, A&A, 617, A144
Huby, Baudoz, Mawet, & Absil. 2015, A&A, 584, A74
Huby, Bottom, Femenia, et al. 2017, A&A, 600, A46
Jackson, Wyatt, Bonsor, & Veras. 2014, MNRAS, 440, 3757
Janson, Carson, Thalmann, et al. 2011, ApJ, 728, 85
Keppler, Benisty, Müller, et al. 2018, A&A, 617, A44
Keppler, Teague, Bae, et al. 2019, arXiv.org 1902.07639
Kervella, Lagadec, Montargès, et al. 2016, A&A, 585, A28
Kervella, Montargès, Lagadec, et al. 2015, A&A, 578, A77
Khorrami, Lanz, Vakili, et al. 2016, A&A, 588, L7
Khorrami, Vakili, Lanz, et al. 2017, A&A, 602, A56
Khouri, Maercker, Waters, et al. 2016, A&A, 591, A70
Khouri, Vlemmings, Olofsson, et al. 2018, A&A, 620, A75
Konopacky, Barman, Macintosh, & Marois. 2013, Science, 339, 1398
Kral, Thébault, Augereau, Boccaletti, & Charnoz. 2015, A&A, 573, A39
Kuzuhara, Tamura, Kudo, et al. 2013, ApJ, 774, 11
Lagrange, Boccaletti, Langlois, et al. 2019, A&A, 621, L8
Lagrange, Gratadour, Chauvin, et al. 2009, A&A, 493, L21
Lagrange, Keppler, Meunier, et al. 2018, A&A, 612, A108
Lagrange, Langlois, Gratton, et al. 2016, A&A, 586, L8
Lamb, Correia, Sauvage, et al. 2017, Journal of Astronomical Telescopes, Instruments, and Systems, 3, 039001
Lannier, Lagrange, Bonavita, et al. 2017, A&A, 603, A54
Lawson, Belikov, Cash, et al. 2013, in Proc. SPIE, Vol. 8864, Techniques and Instrumentation for Detection of Exoplanets VI, 88641F
Lee & Chiang. 2016, ApJ, 827, 125
Li Causi, Stangalini, Antoniucci, et al. 2017, ApJ, 849, 85
Ligi, Vigan, Gratton, et al. 2018, MNRAS, 473, 1774
Lovis, Snellen, Mouillet, et al. 2017, A&A, 599, A16
Machida, Kokubo, Inutsuka, & Matsumoto. 2010, MNRAS, 405, 1227
Macintosh, Chilcote, Bailey, et al. 2018, in Proc. SPIE, Vol. 10703, Adaptive Optics Systems VI, 107030K
Macintosh, Graham, Ingraham, et al. 2014, Proceedings of the National Academy of Science, 111, 12661
Maire, Bonnefoy, Ginski, et al. 2016, A&A, 587, A56
Maire, Rodet, Lazzoni, et al. 2018, A&A, 615, A177

Marois, Lafrenière, Doyon, Macintosh, & Nadeau. 2006, ApJ, 641, 556
Marois, Macintosh, & Véran. 2010, in Proc. SPIE, Vol. 7736, Adaptive Optics Systems II, 77361J
Marsset, Carry, Dumas, et al. 2017, A&A, 604, A64
Martinache. 2013, PASP, 125, 422
Martinache, Guyon, Jovanovic, et al. 2014, Publications of the Astronomical Society of the Pacific, 126, 565
Martinache, Jovanovic, & Guyon. 2016, A&A, 593, A33
Martinez, Kasper, Costille, et al. 2013, A&A, 554, A41
Martinez, Loose, Aller Carpentier, & Kasper. 2012, A&A, 541, A136
Matthews, Crepp, Vasisht, & Cady. 2017, Journal of Astronomical Telescopes, Instruments, and Systems, 3, 045001
Mattioli, Pedichini, Antoniucci, et al. 2019, Research Notes of the American Astronomical Society, 3, 20
Mawet, Bond, Delorme, et al. 2018, in Proc. SPIE, Vol. 10703, Adaptive Optics Systems VI, 1070306
Mawet, Pueyo, Moody, Krist, & Serabyn. 2010, in Proc. SPIE, Vol. 7739, Modern Technologies in Space- and Ground-based Telescopes and Instrumentation, 773914
Mawet, Riaud, Baudrand, et al. 2006, A&A, 448, 801
Mayor & Queloz. 1995, Nature, 378, 355
Mesa, Baudino, Charnay, et al. 2018, A&A, 612, A92
Mesa, Vigan, D'Orazi, et al. 2016, A&A, 593, A119
Milli, Banas, Mouillet, et al. 2016, in Adaptive Optics Systems V, Vol. 9909, 99094Z
Milli, Engler, Schmid, et al. 2019, arXiv.org 1905.03603
Milli, Kasper, Bourget, et al. 2018, in Proc. SPIE, Vol. 10703, Adaptive Optics Systems VI, 107032A
Milli, Vigan, Mouillet, et al. 2017, A&A, 599, A108
Mordasini, Marleau, & Mollière. 2017, A&A, 608, A72
Mouillet, Larwood, Papaloizou, & Lagrange. 1997, MNRAS, 292, 896
Mouillet, Milli, Sauvage, et al. 2018, in Proc. SPIE, Vol. 10703, Adaptive Optics Systems VI, 107031Q
Müller, Keppler, Henning, et al. 2018, A&A, 617, L2
Nakajima, Oppenheimer, Kulkarni, et al. 1995, Nature, 378, 463
N'Diaye, Dohlen, Fusco, & Paul. 2013, A&A, 555, A94
N'Diaye, Martinache, Jovanovic, et al. 2018, A&A, 610, A18
N'Diaye, Vigan, Dohlen, et al. 2016, A&A, 592, A79
Ohnaka, Weigelt, & Hofmann. 2016, A&A, 589, A91
Ohnaka, Weigelt, & Hofmann. 2017, A&A, 597, A20
Olofsson, Samland, Avenhaus, et al. 2016, A&A, 591, A108
Otten, Snik, Kenworthy, et al. 2017, ApJ, 834, 175
Paul, Sauvage, & Mugnier. 2013, A&A, 552, A48
Paul, Sauvage, Mugnier, et al. 2014, A&A, 572, A32
Pedichini, Stangalini, Ambrosino, et al. 2017, , 154, 74
Perrot, Boccaletti, Pantin, et al. 2016, A&A, 590, L7
Pohl, Benisty, Pinilla, et al. 2017, ApJ, 850, 52
Por. 2017, in Proc. SPIE, Vol. 10400, Society of Photo-Optical Instrumentation Engineers (SPIE) Conference Series, 104000V
Por & Haffert. 2018, arXiv.org 1802.10691
Racine, Walker, Nadeau, Doyon, & Marois. 1999, PASP, 111, 587
Rameau, Chauvin, Lagrange, et al. 2013, ApJ, 772, L15
Rouan, Riaud, Boccaletti, Clénet, & Labeyrie. 2000, PASP, 112, 1479
Ruffio, Macintosh, Wang, et al. 2017, ApJ, 842, 14
Samland, Mollière, Bonnefoy, et al. 2017, A&A, 603, A57

Sauvage, Fusco, Lamb, et al. 2016, in , 990916
Savransky, Macintosh, Thomas, et al. 2012, in Proc. SPIE, Vol. 8447, Adaptive Optics Systems III, 84476S
Schmid, Bazzon, Milli, et al. 2017, A&A, 602, A53
Schmid, Bazzon, Roelfsema, et al. 2018, A&A, 619, A9
Scicluna, Siebenmorgen, Wesson, et al. 2015, A&A, 584, L10
Seager & Deming. 2010, ARA&A, 48, 631
Sezestre, Augereau, Boccaletti, & Thébault. 2017, A&A, 607, A65
Singh, Lozi, Guyon, et al. 2015, PASP, 127, 857
Sissa, Olofsson, Vigan, et al. 2018, A&A, 613, L6
Snellen, de Kok, Birkby, et al. 2015, Astronomy & Astrophysics, 576, A59
Snellen, Brandl, de Kok, et al. 2014, Nature, 509, 63
Snellen, Brandl, de Kok, et al. 2014, Nature, 509, 63
Soulain, Millour, Lopez, et al. 2018, A&A, 618, A108
Soummer. 2005, ApJ, 618, L161
Sparks & Ford. 2002, The Astrophysical Journal, 578, 543
Stangalini, Pedichini, Pinna, et al. 2017, Journal of Astronomical Telescopes, Instruments, and Systems, 3, 025001
Stevenson, Harrington, Nymeyer, et al. 2010, Nature, 464, 1161
Stolker, Dominik, Avenhaus, et al. 2016, A&A, 595, A113
Tremblin, Amundsen, Mourier, et al. 2015, ApJ, 804, L17
van Boekel, Henning, Menu, et al. 2017, ApJ, 837, 132
van Holstein, Snik, Girard, et al. 2017, in Proc. SPIE, Vol. 10400, Society of Photo-Optical Instrumentation Engineers (SPIE) Conference Series, 1040015
Vernazza, Brož, Drouard, et al. 2018, A&A, 618, A154
Vigan, Bonavita, Biller, et al. 2017, A&A, 603, A3
Vigan, Bonnefoy, Ginski, et al. 2016, A&A, 587, A55
Vigan, N'Diaye, Dohlen, et al. submitted, A&A
Vigan, Otten, Muslimov, et al. 2018, in Proc. SPIE, Vol. 10702, Ground-based and Airborne Instrumentation for Astronomy VII, 1070236
Viikinkoski, Kaasalainen, Ďurech, et al. 2015, A&A, 581, L3
Viikinkoski, Vernazza, Hanuš, et al. 2018, A&A, 619, L3
Wagner, Follette, Close, et al. 2018, ApJ, 863, L8
Wahhaj, Milli, Kennedy, et al. 2016, A&A, 596, L4
Wilby, Keller, Sauvage, et al. 2018, A&A, 615, A34
Wilby, Keller, Snik, Korkiakoski, & Pietrow. 2017, A&A, 597, A112
Zhou, Herczeg, Kraus, Metchev, & Cruz. 2014, ApJ, 783, L17
Zuckerman & Becklin. 1992, ApJ, 386, 260
Zurlo, Gratton, Mesa, et al. 2018, MNRAS, 480, 236
Zurlo, Vigan, Galicher, et al. 2016, A&A, 587, A57